JOURNAL OF GEOPHYSICAL RESEARCH: SPACE PHYSICS, VOL. 118, 3096–3112, doi:10.1002/jgra.50349, 2013

Analytical estimates of electron quasi-linear diffusion by fast magnetosonic waves

D. Mourenas,[1] A. V. Artemyev,[2,3] O. V. Agapitov,[2,4] and V. Krasnoselskikh[2]

Received 14 March 2013; revised 18 April 2013; accepted 20 May 2013; published 14 June 2013.

[1] Quantifying the loss of relativistic electrons from the Earth's radiation belts requires to estimate the effects of many kinds of observed waves, ranging from ULF to VLF. Analytical estimates of electron quasi-linear diffusion coefficients for whistler-mode chorus and hiss waves of arbitrary obliquity have been recently derived, allowing useful analytical approximations for lifetimes. We examine here the influence of much lower frequency and highly oblique, fast magnetosonic waves (also called ELF equatorial noise) by means of both approximate analytical formulations of the corresponding diffusion coefficients and full numerical simulations. Further analytical developments allow us to identify the most critical wave and plasma parameters necessary for a strong impact of fast magnetosonic waves on electron lifetimes and acceleration in the simultaneous presence of chorus, hiss, or lightning-generated waves, both inside and outside the plasmasphere. In this respect, a relatively small frequency over ion gyrofrequency ratio appears more favorable, and other propitious circumstances are characterized. This study should be useful for a comprehensive appraisal of the potential effect of fast magnetosonic waves throughout the magnetosphere.

Citation: Mourenas, D., A. V. Artemyev, O. V. Agapitov, and V. Krasnoselskikh (2013), Analytical estimates of electron quasi-linear diffusion by fast magnetosonic waves, *J. Geophys. Res. Space Physics*, *118*, 3096–3112, doi:10.1002/jgra.50349.

1. Introduction

[2] The Van Allen radiation belts exhibit intense relativistic electron fluxes during geomagnetically disturbed periods, representing a potential hazard to sensitive satellite electronics [*Iucci et al.*, 2005; *Choi et al.*, 2011]. This fact has led to a growing interest in "space weather" forecasting [e.g., see *Barker et al*., 2005]. However, many different acceleration and loss mechanisms may act simultaneously [*Thorne*, 2010]. Multidimensional codes developed to simulate the dynamics of the radiation belts aim ultimately at incorporating all the needed physical processes [*Barker et al.*, 2005; *Varotsou et al.*, 2008; *Xiao et al.*, 2009; *Fok et al.*, 2011; *Kim et al.*, 2011; *Reeves et al.*, 2012]. While electron diffusion by hiss, lightning-generated, and oblique chorus whistler-mode waves appears to be one of the main loss and acceleration mechanisms [*Albert*, 2007; *Li et al.*, 2007; *Summers et al.*, 2007; *Shprits et al.*, 2008; *Meredith et al.*, 2009; *Artemyev et al.*, 2012; *Mourenas et al.*, 2012b] together with radial and adiabatic diffusion [e.g., *Ukhorskiy et al*., 2011; *Millan and Baker*, 2012, and references therein], energy (and pitch angle) diffusion by fast magnetosonic waves observed in the equatorial region has recently been shown to be quite efficient too [*Horne et al.*, 2007], giving rise to many different studies [e.g., see *Meredith et al*., 2008, 2009; *Bortnik and Thorne*, 2010; *Chen et al*., 2011; *Liu et al*., 2011; *Shprits et al*., 2013, and references therein].

[3] Fast magnetosonic waves are highly oblique whistler-mode waves observed between the ion gyrofrequency and the lower-hybrid frequency: $\Omega_{ci} \leq \omega < \sqrt{\Omega_{ce}\Omega_{ci}}$ with $\Omega_{pe}^2 \gg \Omega_{ce}^2$, where ω is the wave frequency, and Ω_{ci}, Ω_{ce} and Ω_{pe} are the local ion gyrofrequency, electron gyrofrequency, and plasma frequency, respectively [*Russell et al.*, 1970; *Perraut et al.*, 1982; *Santolík et al.*, 2002; *Němec et al.*, 2005]. Excited by injected proton ring distributions of about 10 keV [*Perraut et al.*, 1982; *Horne et al.*, 2000; *Santolík et al.*, 2002; *Meredith et al.*, 2008; *Chen et al.*, 2011; *Liu et al.*, 2011], they are mainly confined to within 3° of the geomagnetic equator [*Russell et al.*, 1970; *Gurnett*, 1976; *Boardsen et al.*, 1992; *Kasahara et al.*, 1994; *Němec et al.*, 2005]. They are observed inside the plasmasphere mostly in the dusk region and outside of the plasmasphere at nearly all local times, with maximum intensities between $L = 3$ and $L = 6$ but still present from $L \sim 2$ to 9 [*Meredith et al.*, 2008; *Shprits et al.*, 2013]. Out of the plasmasphere, Landau damping by abundant plasmasheet electrons (from 0.1 to 0.5 keV) is expected to limit their propagation to latitudes less than a few degrees, as well as to restrict their wave-normal angles to the very close vicinity of the perpendicular to the geomagnetic field [*Horne et al.*, 2000].

[4] Quasi-linear scattering by resonant interaction with magnetosonic waves is one of the important loss and acceleration processes of trapped electrons [*Thorne*, 2010].

[1]CEA, DAM, DIF, Arpajon, France.
[2]LPC2E/CNRS - University of Orleans, Orleans, France.
[3]Space Research Institute, RAS, Moscow, Russia.
[4]National Taras Shevchenko University of Kiev, Kiev, Ukraine.

Corresponding author: D. Mourenas, CEA, DAM, DIF, F-91297, Arpajon, France. (didier.mourenas@cea.fr)

2169-9380/13/10.1002/jgra.50349

Quasi-linear theory can be used [*Lyons et al*., 1971, 1972; *Lyons*, 1974] in the limit of moderate amplitude broadband waves or for ensemble averages (over many bounce periods) of narrowband waves of varying frequencies, such that particle displacements can be considered stochastic. The applicability of quasi-linear theory to Landau scattering of electrons by fast magnetosonic waves has been demonstrated recently in test-particle simulations by *Bortnik and Thorne* [2010]. However, accurate multidimensional simulations of the whole space- and time-varying radiation belts would require a large number of repeated evaluations of diffusion coefficients, making realistic and accurate simulations very time-consuming. *Summers* [2005] and *Albert* [2007] have therefore proposed two useful approximations based on the selection of a wave-normal angle θ representative of the average over the whole distribution, applicable for moderately oblique hiss and chorus waves. As an even quicker alternative, *Mourenas and Ripoll* [2012] and *Mourenas et al*. [2012b, 2012a] have proposed analytical estimates of the electron diffusion coefficients and lifetimes, which have been shown to be accurate enough for both moderately oblique hiss, lightning, and chorus as well as for very oblique chorus waves and for energies ranging from 0.1 to 5 MeV (see also *Artemyev et al*. [2013]). While the latter work was concerned with oblique hiss and chorus waves, we shall focus here on very oblique fast magnetosonic waves [*Horne et al.*, 2007; *Meredith et al.*, 2008], with a very different dispersion relation.

[5] Notwithstanding the many previous studies of electron diffusion by fast magnetosonic waves [*Horne et al.*, 2007; *Meredith et al.*, 2009; *Bortnik and Thorne*, 2010; *Liu et al.*, 2011; *Shprits et al.*, 2013], the parameter range of strong potential effects of these waves on radiation belt electron lifetimes (and acceleration) has not yet been fully assessed. The purpose of the present paper is twofold: (1) to derive analytical estimates of quasi-linear diffusion coefficients corresponding to fast magnetosonic waves, following methods introduced by *Albert* [2008] and *Mourenas et al.* [2012b]; and (2) based on these analytical results, to determine the parameter domain where electron lifetimes (and acceleration) should be most efficiently modified, via appropriate comparisons with estimates obtained previously for scattering by chorus, hiss, or lightning-generated whistler-mode waves. Quantitative estimates of the lifetime decrease will be likewise formulated.

[6] This study should help to provide a better understanding of the complicated variations of the electron diffusion rate as a function of the different wave and plasma parameters while indicating which parameters are most critical and therefore worth monitoring most closely by radiation belt probes or else in numerical simulations. A simplified model of fast magnetosonic wave power distribution derived from Cluster measurements is first presented in section 2. Next, analytical expressions of the diffusion coefficients are derived, allowing us to circumscribe the parameter domain of potential influence of magnetosonic waves in the presence of other kinds of waves (such as chorus or hiss). In the fourth section, the results of the analytical model are compared to diffusion coefficients obtained from full numerical calculations for realistic wave and plasma parameters. The analytical estimates are found to be in good agreement with the full numerical results. Potential implications for the overall dynamics of the inner and outer radiation belts are also outlined.

2. Simplified Model of Magnetosonic Wave Power Distribution Based on CLUSTER Observations

[7] For this work, we made use of a large data set for ELF/VLF waves, as observed by Cluster between January 2001 and December 2010, in the domain $2 < L < 7$ (for $L > 7$, Cluster statistics for the equatorial region is rather poor). The Cluster data set contains a sufficient number of points for performing a statistical study for the range of MLT and L shells that is discussed. The data set is described in detail in *Agapitov et al*. [2011, 2012]. Our analysis was primarily based on data from the Spatio-Temporal Analysis of Field Fluctuations-Spectrum Analyzer (STAFF-SA) experiment [*Cornilleau-Wehrlin et al.*, 2003], which provides the complete spectral matrix (the real and the imaginary part) of the three magnetic components as measured by the STAFF search coil magnetometer. Our survey included STAFF-SA data from the Cluster 4 spacecraft in order to avoid different statistical contributions due to different cross-spacecraft distances during the processing period. The spectral matrix was computed on-board for 27 frequency channels with central frequencies logarithmically spaced between 8.8 Hz and 3.56 kHz (coverage from 8 Hz to 4kHz). The sensitivity of the STAFF search coil magnetometers was $5\cdot10^{-3}$ nT Hz$^{-1/2}$ at 1 Hz, and $4\cdot10^{-5}$ nT Hz$^{-1/2}$ at 100 Hz and 4 kHz [*Cornilleau-Wehrlin et al.*, 2003]. The analyzed magnetosonic waves have amplitudes greater than 1 pT in the wave frequency range from the proton gyrofrequency $f_{ci} = \Omega_{ci}/2\pi$ up to the lower-hybrid frequency $f_{\rm LH} \approx \sqrt{\Omega_{ci}\Omega_c}/2\pi$. This range is known to be dominated by equatorial electromagnetic noise [*Laakso et al.*, 1990; *Santolik et al.*, 2002; *Pokhotelov et al.*, 2008]. Magnetosonic waves are concentrated in the MLT range from 10 to 18, and their normals are mainly perpendicular to the background magnetic field. The values of $f_{\rm LH}$ and f_{ci} were computed using the Cluster FGM magnetic field measurements [*Balogh et al.*, 2001]. The data analysis was performed using the singular value decomposition technique [*Santolik et al.*, 2003] for the wave-normal vector evaluation and estimation of polarization.

[8] Figure 1 shows an example of equatorial noise emissions captured by the Cluster 4 spacecraft during a crossing of the geomagnetic equator on 16 September 2003. The magnetic field amplitude integrated in the frequency range from 8 Hz to $f_{\rm LH}$ is shown in Figure 1b. The magnetic and electric wave power are presented in Figures 1c and 1d, respectively. Intense electromagnetic emissions are observed below the lower-hybrid frequency (indicated by dashed line) in two frequency ranges from 30 Hz to 50 Hz and from 80 Hz to 150 Hz. The wave power maximum is observed in the close vicinity of the geomagnetic equator ($|\lambda| < 5°$). The normal angle θ is shown in Figure 1e. Wave normals for magnetosonic waves are close to transverse direction relative to the background magnetic field. The polarization estimated as the ratio of the intermediate and maximal eigen values (l_2/l_1) of magnetic field spectral matrices are shown in Figure 1f. A linear polarization with $l_2/l_1 < 0.1$ is seen for all the magnetosonic frequency range.

[9] The statistics of equatorial noise below the lower-hybrid frequency measured by Cluster 4 during low

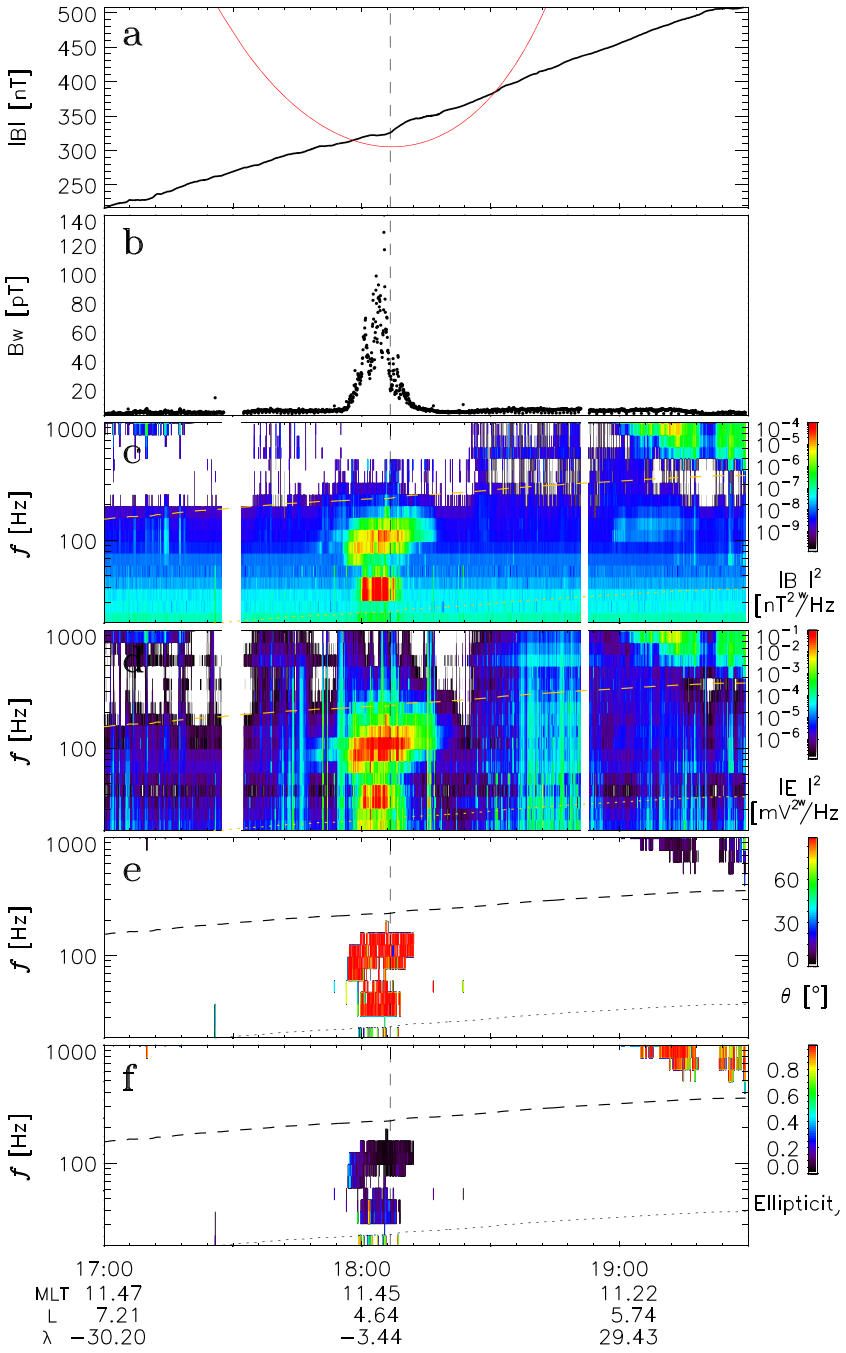

Figure 1. (a) Local magnetic field along the spacecraft trajectory (black) and the model magnetic field along the field line, which is crossed by the spacecraft at the equator. (b) Magnetic field amplitude in the frequency range of magnetosonic waves. (c) Wave magnetic field spectral power. The local value of f_{LH} is indicated by a dashed line, and $5f_{ci}$ is shown by a dotted line. (d) Wave electric field spectral power. (e) Normal angle θ. (f) Ellipticity of magnetic field fluctuations estimated as l_2/l_1.

geomagnetic activity is shown in Figure 2a. One can see a strong maximum around MLT ∼14–15 with amplitudes ∼20–25 pT. Waves concentrate around the geomagnetic equator with a variance $\delta\lambda \sim 3°$ (Figure 2b). While the position of the effective minimum-B equator is actually slightly shifted from the geomagnetic equator (see the example in Figure 1a), comparing Cluster orbits with the Tsyganenko T96 model for $L = 4$ to 5 shows that the distribution of such shifts has a very small mean value $\sim 0.25° < \delta\lambda/10$ as well as a small variance $\sim 0.5° < \delta\lambda/6$. Shifts are smaller at lower L. Thus, the obtained $\delta\lambda$ value should represent a good estimate of the actual latitudinal range where most of the intense fast magnetosonic waves are present.

[10] Based on Cluster measurements between $L = 2.25$ and 5.75, the following approximate numerical fit to the average wave intensities B_w^2 (in units of pT^2) has been

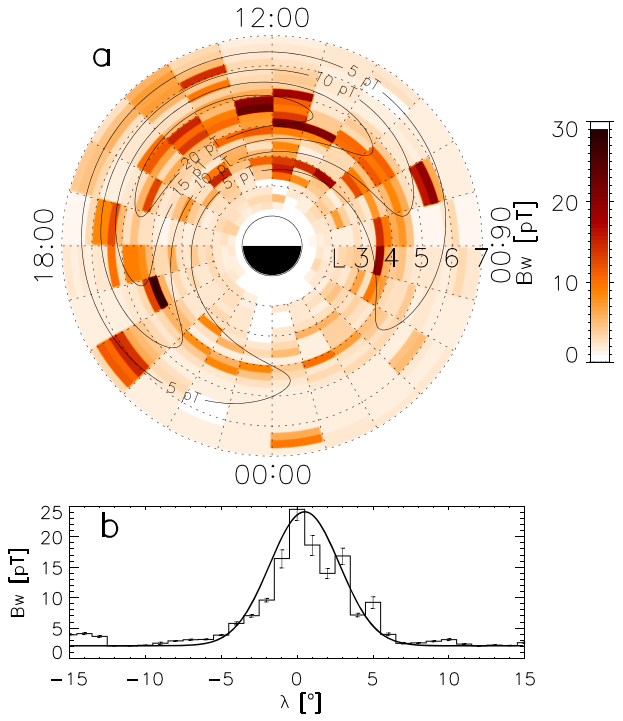

Figure 2. (a) Distribution of magnetosonic waves (square root of average intensity) for low geomagnetic activity ($K_p < 3$). (b) Distribution over magnetic latitude for $L \in [4, 5]$ and MLT from 9 up to 18.

obtained as a function of latitude λ and L after an averaging over magnetic local time:

$$B_w^2 \approx 6 + 23^2 \exp(-\lambda^2/\delta\lambda^2(L)) \exp(-(L-4.5)^2), \quad (1)$$

where $\delta\lambda(L) = 2.5°(1 + L/20)$.

[11] Figure 2 shows both Cluster data and the corresponding numerical fit given by equation (1). The variance value $\delta\lambda \approx 3°$ is in good agreement with previous studies [*Meredith et al.*, 2008]. Averaging equation (1) over both $L = 7$ to 3 and $\lambda = 0$ to 5° yields an average root-mean-square amplitude $\sqrt{\langle B_w^2 \rangle_{L,\lambda}} \sim 10$ pT. In order to compare with THEMIS data, the distribution of amplitudes during Solar minimum provided in Figure 2 in the work by *Shprits et al.* [2013] has been used to calculate roughly the root-mean-square amplitude, giving about 15 pT over approximately the same ranges of L and latitudes. Around $L = 4.5$, realistic root-mean-square amplitudes are slightly larger, about ~ 25 pT.

[12] For the frequency distribution of the waves, unless otherwise stated, we shall consider a Gaussian distribution centered at $\omega_m \sim 7\Omega_{ci}$ as *Horne et al.* [2007] from Cluster observations near $L = 4.5$. Furthermore, we shall use a Gaussian wave-normal angle distribution similar to that of *Horne et al.* [2007], peaked at $\tan\theta_m = \tan 89°$ with a width $\tan\Delta\theta = \tan 86°$ and cutoffs at 88.6° and 89.2°.

3. Analytical Estimates of Diffusion Coefficients for Magnetosonic Waves

[13] The general local pitch angle quasi-linear diffusion coefficient D (in s^{-1}) originally derived by *Lyons* [1974] has been rewritten by *Albert* [2005, 2007] under the form

$$D = \frac{D^{\alpha\alpha}}{p^2} = \frac{\Omega_{ce}}{\gamma^2}\frac{B_w^2}{B^2}\sum_{n=-\infty}^{+\infty}\sum_{\omega} D_n^{\alpha\alpha}$$

$$D_n^{\alpha\alpha} = \int_{\theta_{\min}}^{\theta_{\max}} \sin(\theta)\mathrm{d}\theta \Delta_n G_\omega G_\theta \quad (2)$$

with

$$\Delta_n = \frac{\pi\Phi_n^2}{2\cos\theta|v_\parallel/c|^3}\frac{|\sin^2\alpha + n\Omega_c/\gamma\omega|^2}{|1-(\partial\omega/\partial k_\parallel)_\theta/v_\parallel|} \quad (3)$$

$$G_\omega = \frac{\Omega_{ce}\, B_w^2(\omega)}{\int_{\omega_{LC}}^{\omega_{UC}} B_w^2(\omega')\mathrm{d}\omega'},\ G_\theta(\omega,\theta) = \frac{g(\theta)}{N(\omega,\theta)} \quad (4)$$

$$N(\omega,\theta) = \int_{\theta_{\min}}^{\theta_{\max}} \mathrm{d}\theta' \sin\theta' \Gamma g(\theta')$$

$$\Gamma(\theta', \omega(\theta)) = \mu^2|\mu + \omega\partial\mu/\partial\omega|, \quad (5)$$

where $\mu(\omega,\theta) = kc/\omega$ is the wave refractive index and B the local magnetic field amplitude. Φ_n^2 accounts for the electric and magnetic field components of the wave; it is given in equation (9) of *Lyons* [1974] as a function of Bessel functions J_n with argument $x = \gamma k v \sin\alpha \sin\theta/\Omega_{ce}$, where γ is the relativistic factor and v is the electron velocity. We assume that the spectral density of the fast magnetosonic waves can be written as $B_w^2(\omega) = \exp(-(\omega-\omega_m)^2/\Delta\omega^2)$, with a half-width $\Delta\omega < \omega_m/2$ and lower and upper cutoffs at $\omega_{LC} \approx \omega_m - \Delta\omega$ and $\omega_{UC} \approx \omega_m + \Delta\omega$. Moreover, we take $g(\theta) = \exp(-(\tan\theta - \tan\theta_m)^2/\tan^2\Delta\theta)$. In equation (2), $G_\theta(\omega,\theta)$ and $D_n^{\alpha\alpha}$ are both evaluated at the resonant frequency ω corresponding to a θ and a pitch angle α determined from the Landau resonance condition (i.e., $n = 0$, which has been shown by *Horne et al.* [2007] to be largely predominant for fast magnetosonic waves)

$$\omega = kv\cos\theta\cos\alpha. \quad (6)$$

There may be several roots of ω, hence the sum over ω in equation (2). An important point is that $D_0^{\alpha\alpha}$ and $G_\theta(\omega,\theta)$ depend only on θ. Landau resonance occurs during the bounce motion of electrons from the equator to their mirror point, and the bounce averaging procedure has been described by *Lyons et al.* [1972].

[14] To proceed with analytical calculations, we further assume that the refractive index μ of fast magnetosonic waves can be obtained from the cold plasma dispersion relation for a typical low-β equatorial plasma in the inner magnetosphere, composed of ions and electrons. The following inequalities are usually satisfied for the observed fast magnetosonic waves: $(\omega/\Omega_{ci})^2 > 2$, $\omega^2/(\Omega_{ci}\Omega_{ce}) < 1/2$, $\cos^2\theta \ll (\Omega_{ci}/\omega)^2$, and $\cos\theta < \sqrt{\Omega_{ci}/\Omega_{ce}}$ since $\theta > 88.5°$ [*Russell et al.*, 1970; *Boardsen et al.*, 1992; *Horne et al.*, 2000; *Němec et al.*, 2005; *Horne et al.*, 2007; *Liu et al.*, 2011]. Moreover, $2\Omega_{ci} \le \omega \le 25\Omega_{ci}$ [*Němec et al.*, 2005; *Horne et al.*, 2007; *Chen et al.*, 2011] are generally accepted figures in the terrestrial magnetosphere. Building on the preceding inequalities, the full whistler-mode dispersion relation [*Lyons et al.*, 1971; *Lyons*, 1974] reduces for very oblique fast magnetosonic waves to $\mu^2 \sim RL/S$ with R, L, and S the usual Stix coefficients [*Stix*, 1962]. This leads to

$$\frac{k^2c^2}{\omega^2} \approx \frac{\Omega_{pe}^2}{\Omega_c\Omega_{ci}}\left(1 - \frac{\omega^2}{\Omega_{ce}\Omega_{ci}}\right)^{-1}, \quad (7)$$

which is equivalent to $\omega = kv_A/\sqrt{1+k^2c^2/\Omega_{pe}^2}$ with v_A the Alfven velocity. Note that $k^2c^2/\Omega_{pe}^2 \sim \omega^2/(\Omega_{ce}\Omega_{ci}) \ll 1$ implies that $\omega \approx kv_A$ in practice.

[15] It is worthy of note that fast magnetosonic waves, being generated at harmonics of the ion gyrofrequency, should exhibit (at least locally) a noncontinuous frequency spectrum with clear line structure, differing from the continuous spectra considered in our analytical developments. When considering Landau resonance with these waves, however, the parallel phase velocities $\omega/(k\cos\theta) \sim v_A/(\cos\theta(1+\omega^2/(\Omega_{ce}\Omega_{ci}))^{1/2})$ corresponding to distinct n-harmonic sub-elements $\omega = n\Omega_{ci}$ may overlap, provided that $\tan\Delta\theta/\tan\theta_m > 2n\Omega_{ci0}/\Omega_{ce0}$. Since the latter condition should be easily satisfied, the Chirikov criterion for stochastic motion should be fulfilled, justifying the use of quasi-linear theory for not-too-high wave amplitudes [e.g., see *Shapiro and Sagdeev*, 1997]. In such a situation, considering a continuous frequency spectrum should be a good approximation.

[16] From equations (6) and (7), an expression for the resonant k can be obtained as a function of θ and α:

$$\frac{k^2c^2}{\Omega_{pe}^2} \approx \frac{v_A^2}{v^2\cos^2\alpha\cos^2\theta} - 1, \tag{8}$$

from which the resonant θ value can be written as a function of ω:

$$\cos^2\theta \approx \frac{v_A^2}{v^2\cos^2\alpha} - \frac{c^2\omega^2}{v^2\cos^2\alpha\,\Omega_{pe}^2}. \tag{9}$$

Since magnetosonic waves are such that $\omega^2 \ll \Omega_{ci}\Omega_{ce}$, one has $\omega c \ll \Omega_{pe}v_A$. Consequently, a very good approximation to equation (9) is

$$\cos\theta_r \approx \frac{v_A}{v\cos\alpha}, \tag{10}$$

meaning that θ is an almost constant function of ω, as already apparent in the numerical results of Figure 1 in the work by *Albert* [2008]. In particular, equation (8) shows that both k and ω increase very quickly from zero in the close vicinity of the approximation (10) for the resonant θ. As a result, θ can be considered as nearly fixed: $\theta \sim \theta_r$. To get an accurate analytical estimate of D, it is therefore more appropriate to rewrite the integral over θ in equation (2) as an integral over ω, as already noticed by *Albert* [2008]. Moreover, the resonant value of θ can be taken from equation (10) [i.e., independent of ω: it is essentially equivalent to a Dirac function $\delta(\theta-\theta_r)$]. Since the frequency spectrum is rather narrow, with $\Delta\omega \sim \omega_m/3$ typically [*Horne et al.*, 2007], it is also reasonable to replace the weighted average over ω in equation (9) in the work by *Albert* [2008] by an evaluation at ω_m. Thus, the local D can be estimated from equation (13) in the work by *Albert* [2008] (i.e., the mean value approximation) calculated for ω_m and θ_r:

$$\frac{D_0^{\alpha\alpha}}{p^2} \sim \frac{\Omega_{ce}^2}{\gamma^2}\frac{B_w^2}{B^2}\frac{\Delta_0(\omega_m,\theta_r)\,g(\theta_r)|\mathrm{d}\theta/\mathrm{d}\omega|_r/\Gamma(\omega_m)}{\int_{\theta_{\min}}^{\theta_{\max}}\sin\theta g(\theta)\mathrm{d}\theta} \tag{11}$$

[17] The normalizing integral over θ at the denominator of equation (11) can be approximated to first order by $\sqrt{\pi}\,\mathrm{erf}(1)\tan\Delta\theta/\tan^2\theta_m$ (which is a very good approximation for $\tan\theta_{\min(\max)}$ not too far from $\tan\theta_m \mp \tan\Delta\theta$). Making use of the same inequalities concerning magnetosonic waves frequencies and θ values as before, we get also

$$|1-(\partial\omega/\partial k_\parallel)_\theta/v_\parallel| \approx \frac{\omega_m^2}{\Omega_{ci}\Omega_{ce}}\left(1+\frac{\omega_m^2}{\Omega_{ci}\Omega_{ce}}\right)^{-1} \tag{12}$$

and

$$\Gamma \approx \frac{\Omega_{pe}^3}{\Omega_{ci}^{3/2}\Omega_{ce}^{3/2}}\frac{1+\frac{\omega_m^2}{\Omega_{ci}\Omega_{ce}}}{\left(1-\frac{\omega_m^2}{\Omega_{ci}\Omega_{ce}}\right)^{3/2}}, \tag{13}$$

while

$$\left|\frac{\mathrm{d}\theta}{\mathrm{d}\omega}\right|_r \approx \frac{\omega_m\cos\theta_r}{2\Omega_{ci}\Omega_{ce}}. \tag{14}$$

Moreover, the term Φ_0 in Δ_0 can be approximated as

$$\Phi_0 \sim J_1(x) + J_0(x)\frac{\omega^3\cos\theta_r}{\Omega_{ci}^2\Omega_{ce}\tan\alpha} \tag{15}$$

where $x = \gamma\omega v\sin\alpha/(v_A\Omega_{ce})$, and we assumed again $\cos^2\theta_r \ll \Omega_{ci}^2/\omega^2$. It is worth noting that the second term in equation (15) is smaller than the first one for $\sin\alpha > \sqrt{2/\gamma}(c/v)(\omega_m/\Omega_{ci})(\Omega_{ce}/\Omega_{pe})\sqrt{\Omega_{ci}/\Omega_{ce}}\max(1,x^{3/2})$. The latter condition is almost always satisfied in practice for electron energies $E = 0.1$ to 5 MeV and $\omega_m/\Omega_{ci} < 10$ (provided that a realistic electron-to-proton mass ratio is employed, which may not be always the case in particle simulations). Most often, therefore, one can simply use $\Phi_0 \sim J_1(x)$. Moreover, the smooth and monotonic variation of $J_1(x)$ for $x = 0$ to $x \sim 2$ allows to take $\omega \sim \omega_m$ in the expression of x in this range (i.e., at low energy or density); the weighted average over ω needed to get equation (11) is then roughly equivalent to taking $\omega = \omega_m$ in the Bessel function. But at higher x (> 2), $J_1^2(x)$ becomes nonmonotonic, showing a succession of rather closely spaced zeros and peaks. Assuming in addition that $\Delta\omega/\omega_m > 0.15$ for x to be able to vary sensibly around its mean value, the weighted average over ω in D should yield results corresponding to values of $J_1^2(x)$ never far from its upper envelope value $\sim 2/(\pi x)$. Consequently, J_1 can be reasonably approximated in the ω-averaged equations (11)–(15) by $J_1(\omega_m)$ for $x(\omega_m) \le 2$ and by $(|J_1(\omega_m)| + \sqrt{2/(\pi x)})/2$ for $x(\omega_m) > 2$. The latter approximations will be used throughout the following analytical calculations.

[18] Now, let us turn to the integration over bounce motion between the particle's mirror points. As discussed above, the measured fast magnetosonic waves are confined to within a few degrees of the magnetic equator. Assuming a dipolar geomagnetic field (which is roughly correct as long as $L < 6$), the integrand of the bounce-integral $\langle D\rangle_B$ given by *Lyons et al.* [1972] is proportional to $\cos^2\theta_r(\alpha)J_1^2(\omega_m)g(\theta_r(\alpha))/\omega_m$. From the preceding considerations, it is clear that it is weakly varying with α all over the range where $g(\theta) > 1/e$, corresponding to $\tan\theta_m - \tan\Delta\theta < \tan\theta_r < \tan\theta_m + \tan\Delta\theta$. The bounce integral can therefore be approximated by its integrand evaluated at the equatorial value α_0 of the pitch angle, multiplied by the latitude range $\Delta\lambda$ corresponding to the aforementioned θ range. We get $\Delta\lambda \approx \min(\lambda_{\max},\lambda_+)$ with

$$\lambda_+ = \frac{\sqrt{2}}{3\sin\alpha_0}\sqrt{\max\left(0,1-\frac{v_A^2}{v^2\cos^2\theta_{\min}}-\sin^2\alpha_0\right)} \tag{16}$$

where $\tan\theta_{\min(\max)} = \tan\theta_m \mp \tan\Delta\theta$, and $\lambda_{\max}$ denotes the upper latitude of confined waves. The latter is taken here as $\lambda_{\max} = \delta\lambda$ from equation (1) giving the observed latitude profile of the wave intensity. We also use above v_A evaluated at the equator. This finally yields the following:

$$\frac{\langle D^{\alpha\alpha}_{n=0}\rangle_B}{p^2} \approx \frac{\sqrt{\pi}\,\Delta\lambda\,\Omega^2_{ce0}}{4\mathrm{erf}(1)\gamma^2 T}\frac{B^2_w}{B^2_0}\left(1-\frac{\omega^2_m}{\Omega_{ce0}\Omega_{ci0}}\right)^{3/2} \times \frac{c^3\tan^4\alpha_0\,\Phi^2_0(\alpha_0,\omega_m,\theta_r)\,g(\theta_r)\,\Omega^{3/2}_{ce0}\Omega^{3/2}_{ci0}\tan^2\theta_m}{v^3\omega_m\Omega^3_{pe}\tan\Delta\theta}, \tag{17}$$

with "0" subscripts indicating equatorial values and bounce period $T \sim 1.38 - 0.64\sin^{3/4}\alpha_0$ [*Davidson*, 1976]. It is interesting to note that expressions (11) and (17) vary with dispersion like $\omega|\mathrm{d}\theta/\mathrm{d}\omega|/|1 - (\partial\omega/\partial k_\parallel)_\theta/v_\parallel|$ taken at Landau resonance. The latter ratio is nearly independent of $\partial\mu/\partial\omega$, and it is also weakly dependent on the exact $\partial\mu/\partial\theta$ after averaging over realistic, not-too-narrow θ distributions. Thus, equation (17) is expected to provide an accurate estimate of the diffusion rate, although the α_0 position of peak diffusion can be slightly overestimated at very high $\alpha_0 > 85°$ due to neglected off-equatorial resonances.

[19] *Lyons* [1974] has shown that one may write the local momentum diffusion coefficients as a function of the pitch angle ones. After bounce integration, it is straightforward to find from the same considerations as before that

$$\frac{\langle D^{pp}_0\rangle_B}{\langle D^{\alpha\alpha}_0\rangle_B} \approx \frac{\cos^2\alpha_0}{\sin^2\alpha_0}. \tag{18}$$

The energy diffusion coefficients can be easily obtained from the relation $D^{EE}/E^2 = (1+\gamma^{-1})^2 D^{pp}/p^2$ [*Glauert and Horne*, 2005].

[20] Both the wave-normal angle distribution $g(\theta)$ and the frequency distribution of the magnetosonic wave power being taken as narrow Gaussians, it is easy to derive from equation (8) approximate expressions for both the lower-bound $\alpha_{0,\min}$ and the upper-bound $\alpha_{0,\max}$ of significant pitch angle diffusion, as well as the position α_{0M} of its maximum:

$$\begin{aligned}
\cos\alpha_{0M} &\approx \frac{c\sqrt{\Omega_{ce0}\Omega_{ci0}}}{v\Omega_{pe}\cos\theta_m}\left(1+\frac{\omega^2_m}{\Omega_{ce0}\Omega_{ci0}}\right)^{-1/2}\\
\cos\alpha_{0,\max} &\approx \frac{c\sqrt{\Omega_{ce0}\Omega_{ci0}}}{v\Omega_{pe}\cos\theta_{\min}}\left(1+\frac{(\omega_m+\Delta\omega)^2}{\Omega_{ce0}\Omega_{ci0}}\right)^{-1/2}\\
\cos\alpha_{0,\min} &\approx \frac{c\sqrt{\Omega_{ce0}\Omega_{ci0}}}{v\Omega_{pe}\cos\theta_{\max}}\left(1+\frac{(\omega_m-\Delta\omega)^2}{\Omega_{ce0}\Omega_{ci0}}\right)^{-1/2}
\end{aligned} \tag{19}$$

Bounds given in equation (19) will be used together with equation (17) for estimates.

[21] Taking $\alpha_0 = \alpha_{0M}$ in equation (17), the peak magnitude of the pitch angle diffusion rate is found to increase with energy at low energy, varying roughly like $(v/c)^3\cos^2\theta_m\Omega^3_{pe}\omega_m/\left(\Omega^{5/2}_{ce0}\Omega^{3/2}_{ci0}\right)$. It reaches a maximum just before the peak of $\Phi^2_0 \sim J^2_1(x)$ for $x \approx 1$ to 1.8, i.e., for $\gamma v/c \approx \Omega^{3/2}_{ce0}\Omega^{1/2}_{ci0}/(\Omega_{pe}\omega_m)$. It decreases at higher energy, varying then like $\cos^2\theta_m\Omega^2_{ce0}\left(1-\omega^2_m/[\Omega_{ce0}\Omega_{ci0}]\right)^{3/2}/\left(\omega^2_m\gamma^3\right)$.

[22] Finally, for a plasma consisting of multiple ion species i (such as protons, He^+, and O^+), the dispersion relation of the fast magnetosonic mode is slightly modified. Then, the effective Alfven speed becomes $v_A \approx c(\Omega_{ce0}/\Omega_{pe})\sqrt{\sum_s n_s m_e/(n_e m_s)}$ with n_s and m_s the density and mass of species s and $\sum_s n_s = n_e$. Assuming that $n_i < n_p/3$ for all the heavier ion species (with protons denoted by subscript p), one finds approximately $v_A \approx c\sqrt{\Omega_{ce0}\Omega_{cp0}n_p/n_e}/\Omega_{pe}$. In such a case, the above formulas for the diffusion rates can still be used provided that Ω_{ci0} is replaced by $\Omega_{cp0}n_p/n_e$. As a result, including heavier ions leads to an increase of α_{0M}, as well as an increase of the diffusion rate at low energy (i.e., before the peak of Φ^2_0). This is in good agreement with the results of numerical simulations performed by *Shprits et al.* [2013] using different compositions of the plasma expected to correspond to different phases of geomagnetic storms.

4. Parameter Range for a Significant Impact of Fast Magnetosonic Waves

4.1. Effect on Electron Lifetimes

[23] Knowing the maximum value $\langle D^{\alpha\alpha}\rangle_B(\alpha_{0M})$ of the pitch angle diffusion coefficient for fast magnetosonic waves and its range in α_0, one can easily compare the magnitude of pitch angle diffusion by magnetosonic waves to diffusion by other kinds of whistler-mode waves such as hiss, lightning-generated waves, VLF, or chorus, making use of previously derived analytical expressions for the corresponding diffusion coefficients [*Artemyev et al.*, 2013; *Mourenas and Ripoll*, 2012; *Mourenas et al.*, 2012a, 2012b]. While fast magnetosonic waves alone do not lead directly to electron losses [*Horne et al.*, 2007], the additional presence of hiss, lightning-generated, or chorus waves allows electron scattering into the loss cone. In such a realistic situation, magnetosonic waves may decrease particle lifetimes by increasing the total pitch angle diffusion rate over a limited pitch angle domain.

[24] Let us consider successively locations closer and closer to the Earth. Outside the plasmapause for $L > 5.5$, chorus waves are usually dominant, and they seem to be mainly weakly oblique in this domain [*Agapitov et al.*, 2012; *Artemyev et al.*, 2013; *Chen et al.*, 2013]. In such a case, the pitch angle diffusion coefficient for chorus waves $D^{\alpha\alpha}_{CH}$ is close to the parallel approximation one [*Summers et al.*, 2007], and it increases with α_0. Then, the contribution to the electron lifetime integral $\tau \sim \int \mathrm{d}\alpha_0/\left(D^{\alpha\alpha}_{CH}\tan\alpha_0\right)$ [*Albert and Shprits*, 2009] for diffusion by chorus waves is largest at $\alpha_0 < \alpha_{0,\min} \geq 25°$ for $E > 100$ keV and $\Omega_{pe}/\Omega_{ce0} > 3$. Magnetosonic waves should then have little (if any) effect on the lifetimes. Closer to the plasmapause for $4 < L < 5.5$, chorus waves have still been observed to be dominant but with a substantial portion (10% to 20%) of the wave power in very oblique waves, between the Gendrin and resonance cone angles [*Agapitov et al.*, 2012; *Artemyev et al.*, 2013]. An analytical approximate expression for the corresponding diffusion coefficient is $\langle D^{\alpha\alpha}_{CH}\rangle_B/p^2 \approx \left(2\sqrt{8}/9\right)(B_{w,CH}/B_0)^2\Omega^2_{ce0}/(\gamma p\Omega_{pe}\sin\alpha_0)$ [*Mourenas et al.*, 2012b], where p is the momentum normalized to $m_e c$. It is worth noting that the diffusion rate for oblique chorus diminishes toward large α_0. This makes it possible for magnetosonic waves to play an important role, provided that their diffusion rate is higher than the chorus one. In such a case, the electron lifetime will be decreased. Taking

for simplicity $\alpha_0 \approx \alpha_{0M}$, this can occur for high enough magnetosonic wave intensity such that

$$\frac{B_w^2}{B_{w,CH}^2} > \frac{8\sqrt{8}c^2}{9\sqrt{\pi}v^2}\frac{\omega_m\Omega_{ce0}^{1/2}\Omega_{ci0}^{1/2}}{\Delta\lambda\Omega_{pe}^2}\frac{\tan\Delta\theta/\cos^2\theta_m}{\sin^5\alpha_{0M}\Phi_0^2(\theta_r,\alpha_{0M},\omega_m)}. \quad (20)$$

From equations (20) and (15), it is easier for small values of θ_m and $\Delta\theta$, large ratio Ω_{pe}/Ω_{ce0}, and at electron energy and ω_m/Ω_{ce0} values where $\Phi_0^2 \sim J_1^2(x)$ is the largest, i.e., for $(\gamma v/c)(\omega_m/\Omega_{ce0})\sin\alpha_{0M} \approx \sqrt{\Omega_{ce0}\Omega_{ci0}}/\Omega_{pe}$. However, it is worth noting that the eventual reduction of the lifetime is also proportional to the width of the diffusion peak of magnetosonic waves (due to the integral over α_0 in the expression of τ). The latter width is roughly proportional to the θ width of the wave distribution (e.g., see equation (19)). As a result, lifetime reduction is expected to be rather insensitive to $\Delta\theta$ while being strongly dependent on θ_m and ω_m/Ω_{ce0}.

[25] Accurate experimental measurements of the wave-normal angle distribution and frequency distribution of fast magnetosonic waves appear therefore crucial in order to evaluate the role they could play in electron losses at $L \sim 4$ to 5.5 (both outside and inside of the plasmasphere). Since precise measurements of highly oblique wave-normal angles are difficult to achieve, numerical simulations of fast magnetosonic wave generation [*Liu et al.*, 2011] might be a worthy alternative, provided that the correct electron-to-proton mass ratio can be used. It is also worth pointing out that, for fixed θ_m and ω_m/Ω_{ce0}, the reduction of lifetimes at $L = 4$ to 5.5 by magnetosonic waves could be much more important in higher Ω_{pe}/Ω_{ce0} regions where pitch angle diffusion of electrons by chorus waves is reduced while diffusion by magnetosonic waves is increased.

[26] Well inside the plasmasphere, for $L < 3.5$, hiss and lightning-generated whistlers are usually considered to be the most important waves for electron pitch angle diffusion, although it is also widely acknowledged that intense enough VLF and magnetosonic waves may also have some impact on loss timescales [*Meredith et al.*, 2009]. Let $\alpha_{UC,\mathrm{H}} = \arccos\min\left(1, \Omega_{ce0}^{3/2}\left(p\Omega_{pe}\omega_{UC,\mathrm{H}}^{1/2}\right)^{-1}\right)$ denote the upper bound of cyclotron diffusion for hiss waves [see *Artemyev et al.*, 2013] (hereafter, subscripts H indicate hiss variables). If $45° < \alpha_{0M} < \alpha_{UC,\mathrm{H}}$ and hiss waves are weakly oblique for $\lambda < 10°$ (i.e., $\Delta\theta_\mathrm{H} < 45°$ and $\theta_{m,\mathrm{H}} \sim 0$), then adding magnetosonic waves merely increases the largest part (the peak) of the (hiss) cyclotron diffusion coefficient. Consequently, only a very small reduction of lifetimes can then be obtained. Lightning-generated whistler-mode waves are also present in general at $L < 3$, at higher frequencies than hiss waves. Since they are typically much less intense than hiss [*Meredith et al.*, 2009], however, their diffusion rate at $\alpha_0 < \alpha_{UC,\mathrm{H}}$ remains negligible as compared to hiss diffusion. But for $\alpha_{UC,\mathrm{H}} < \alpha_{0M} < \alpha_{UC,\mathrm{LG}}$ (where subscript LG denotes lightning-generated waves), their cyclotron diffusion coefficient dominates over the hiss cyclotron and Landau ones, filling the gap in diffusion between the Landau peak and the first cyclotron peak of hiss [*Meredith et al.*, 2009; *Artemyev et al.*, 2013]. If magnetosonic waves are present in this particular range of pitch angles, they may increase the diffusion rate at the location of one of its minima (different minima may exist: at the loss cone for $\alpha_0 = \alpha_{LC}$, between $\alpha_{UC,\mathrm{H}}$ and $\alpha_{UC,\mathrm{LG}}$, and also above $\alpha_{UC,\mathrm{LG}}$). Thus, they could reduce lifetimes significantly in this case. The minimum magnetosonic to lightning-generated wave power ratio required for magnetosonic wave Landau diffusion to be stronger than lightning-generated wave cyclotron diffusion (given by equation (30) in the work by *Mourenas and Ripoll* [2012]) in this range is

$$\frac{B_{w,\min1}^2}{B_{w,\mathrm{LG}}^2} \approx \frac{4c^2}{\pi v^2}\frac{\omega_m\Omega_{ce0}\Omega_{ci0}^{1/2}}{\Delta\lambda\Omega_{pe}^2\omega_{m,\mathrm{LG}}^{1/2}}\frac{\cos^{-2}\theta_m(\tan\Delta\theta/\tan\Delta\theta_\mathrm{LG})}{\sin^5\alpha_{0M}\Phi_0^2(\theta_r,\alpha_{0M},\omega_m)}. \quad (21)$$

[27] A reduction of lifetimes can be more easily obtained for small values of θ_m (while being relatively insensitive to $\Delta\theta$ for the same reason as stated before), large ratio Ω_{pe}/Ω_{ce0}, and at electron energy and ω_m/Ω_{ce0} values where Φ_0^2 is near its peak value, i.e., for $(\gamma v/c)(\omega_m/\Omega_{ce0})\sin\alpha_{0M} \approx \sqrt{\Omega_{ce0}\Omega_{ci0}}/\Omega_{pe}$. It is interesting to note that the minimum magnetosonic to lightning-generated wave power ratio (21) is larger than the minimum magnetosonic to oblique chorus power ratio (20) by roughly a factor $\sqrt{\Omega_{ce0}/\omega_{m,\mathrm{LG}}}/\tan\Delta\theta_\mathrm{LG} > 2$. However, lightning-generated waves are usually sensibly less intense than the chorus waves observed outside of the plasmapause. At still higher values $\alpha_{0M} > \alpha_{UC,\mathrm{LG}}$, finally, the magnetosonic diffusion rate competes with the Landau diffusion rate from hiss, which is given by equation (34) in the work by *Mourenas and Ripoll* [2012]. An important reduction of lifetimes may again be obtained, requiring a minimum wave power ratio

$$\frac{B_{w,\min2}^2}{B_{w,\mathrm{H}}^2} \approx \frac{4c^2}{\pi\gamma v^2}\frac{\omega_m\Omega_{ce0}^2}{\Delta\lambda\Omega_{pe}^2\Omega_{ci0}}\frac{g_\mathrm{H}\cos\theta_m(\tan\Delta\theta/\tan\Delta\theta_\mathrm{H})}{\sin^4\alpha_{0M}\Phi_0^2(\theta_r,\alpha_{0M},\omega_m)}, \quad (22)$$

where $g_\mathrm{H} = \exp(-1.84^2/z^2) + \min(z^3/11, 1/z)$ for a Gaussian wave-normal angle distribution of hiss waves, with $z = p\varepsilon_\mathrm{H}\tan\Delta\theta_\mathrm{H}$ and $\varepsilon_\mathrm{H} = \sqrt{\omega_{m,\mathrm{H}}/\Omega_{ce0}}\Omega_{pe}/\Omega_{ce0}$ (see details in *Artemyev et al.* [2013]). It is worth emphasizing that an eventual reduction of lifetimes occurs more easily now for larger values of θ_m, contrary to the preceding cases. Nevertheless, relatively large energy, large Ω_{pe}/Ω_{ce0}, and ω_m/Ω_{ce0} values such that $(\gamma v/c)(\omega_m/\Omega_{ce0})\sin\alpha_{0M} \approx \sqrt{\Omega_{ce0}\Omega_{ci0}}/\Omega_{pe}$ are again favorable. Comparing equations (22) and (21) shows an important feature: the minimum wave power ratio is now much smaller than before, by a factor $< \cos^3\theta_m\Omega_{ce0}\omega_{m,\mathrm{LG}}^{1/2}/\left(\Omega_{ci0}^{3/2}\gamma\right) \ll 1$. Since lightning-generated waves are much less intense than hiss in general, it looks like similar levels of magnetosonic waves could impact lifetimes by increasing diffusion almost anywhere in the large pitch angle domain $\alpha_0 > \alpha_{UC,\mathrm{H}}$.

[28] Nevertheless, for magnetosonic waves to make lifetime τ sensibly smaller, they must also fill a sufficiently deep minimum at such large α_0 in the weighted pitch angle diffusion rate $\langle D_{w/o}\rangle_B\tan\alpha_0$ calculated without them [*Albert and Shprits*, 2009]. Consequently, α_{0M} and $\alpha_{UC,\mathrm{H}}$ must not be too large. A prerequisite for a significant reduction of lifetimes by magnetosonic waves is that

$$\frac{\tan\alpha_{0M}}{\tan\alpha_{LC}} < \min\left(\frac{\langle D_\mathrm{H}\rangle_B(\alpha_{LC})}{\langle D_\mathrm{H}\rangle_B(\alpha_{0M})}, \frac{\langle D_\mathrm{H}\rangle_B(\alpha_{LC})}{\langle D_\mathrm{LG}\rangle_B(\alpha_{0M})}\right) \quad (23)$$

This additional constraint in turn increases the minimum needed wave power ratios (21) and (22) by imposing respectively that (for not-too-small energy)

$$\tan\alpha_{0M} < \frac{\gamma B_{w,\mathrm{H}}^2 \Omega_{ce0}^{7/4} \tan\alpha_{LC} \tan\Delta\theta_{\mathrm{LG}}}{36 p^{1/2} B_{w,\mathrm{LG}}^2 \Omega_{pe}^{1/2} \omega_{m,\mathrm{LG}}^{1/2} \omega_{m,\mathrm{H}}^{3/4}},$$
$$\cos\alpha_{0M} < \frac{c\Omega_{ce0}^{3/2}}{\gamma v \Omega_{pe} \omega_{UC,\mathrm{H}}^{1/2}} \quad (24)$$

$$\cos\alpha_{0M} > \frac{2^{1/2} 3^{5/8} \gamma^{1/4} \omega_{m,\mathrm{H}}^{5/18} \Omega_{ce0}^{1/6}}{\pi^{3/8} p^{4/9} \Omega_{pe}^{4/9} \tan^{1/4}\alpha_{LC} \tan^{1/4}\Delta\theta_{\mathrm{H}}},$$
$$\cos\alpha_{0M} < \frac{c\Omega_{ce0}^{3/2}}{\gamma v \Omega_{pe} \omega_{UC,\mathrm{LG}}^{1/2}}. \quad (25)$$

From the different variations with energy of the two opposite limits in each case, it can be seen that the two above α_{0M} ranges shrink to zero at high enough energy: then, it becomes impossible to get any significant decrease of lifetimes due to fast magnetosonic waves. Thus, a decrease can only be obtained over some range of intermediate energies. The last inequalities in (24) and (25) can be rewritten with the help of equation (19) as follows:

$$\gamma < \frac{\Omega_{ce0}\cos\theta_m}{\sqrt{\Omega_{ci0}\omega_{UC}}} \sqrt{1 + \frac{\omega_m^2}{\Omega_{ce0}\Omega_{ci0}}},\ \omega_{UC} = \omega_{UC,\mathrm{LG}}, \omega_{UC,\mathrm{H}}.$$

This condition is satisfied for $\gamma \leq 10$.

[29] The new lifetime τ_w, calculated with fast magnetosonic waves included, is then smaller than the lifetime $\tau_{w/o}$ calculated without them, and it can be expressed under the following form [*Albert and Shprits*, 2009; *Mourenas and Ripoll*, 2012]:

$$\tau_w \approx \tau_{w/o} - \int_{\alpha_1}^{\alpha_2} \frac{B_w^2}{B_w^2 + B_{w,\min}^2} \frac{\mathrm{d}\alpha_0}{\tan\alpha_0 \langle D_{w/o}\rangle_B} \quad (26)$$

where $\alpha_1 = \max(\alpha_{UC,\mathrm{H}}, \alpha_{0,\min})$ and $\alpha_2 = \max(\alpha_{UC,\mathrm{H}}, \alpha_{0,\max})$, while $D_{w/o}$ is D_{H} (for Landau resonance) when $\alpha_0 > \alpha_{UC,\mathrm{LG}}$ and D_{LG} (for cyclotron resonance) when $\alpha_0 < \alpha_{UC,\mathrm{LG}}$, respectively, for $L < 3.5$. Whenever the domain $[\alpha_1, \alpha_2]$ is broad enough around $\alpha_{UC,\mathrm{LG}}$, one should take $B_{w,\min} = B_{w,\min 1}$ for $\alpha_0 < \alpha_{UC,\mathrm{LG}}$ and $B_{w,\min} = B_{w,\min 2}$ for $\alpha_0 > \alpha_{UC,\mathrm{LG}}$. For $L \sim 4$ to 5.5, $B_{w,\min}$ is given by equation (20) instead, with $D_{w/o} = D_{CH}$ and $\alpha_{UC} = 0$ in α_1 and α_2.

[30] Equation (26) can be easily integrated analytically using previously derived diffusion coefficient expressions for hiss and chorus waves [*Mourenas et al.*, 2012b; *Mourenas and Ripoll*, 2012; *Artemyev et al.*, 2013], with the additional assumption that $\alpha_0 > \pi/2 - \Delta\theta_{\mathrm{LG}}$ when $\alpha_0 < \alpha_{UC,\mathrm{LG}}$. An important decrease of electron lifetimes can be induced by fast magnetosonic waves intense enough over a given parameter range. Such a situation occurs at not-too-large energies, in order for $\alpha_{UC,\mathrm{H}}$ and $\alpha_{UC,\mathrm{LG}}$ to be not too high. In such a case, the presence of fast magnetosonic waves could fill a gap in diffusion rate, strongly reducing the lifetimes as shown numerically in one case study by *Meredith et al.* [2009]. However, we hasten to add that very intense magnetosonic waves ($\sqrt{B_w^2} > 200$ pT) seem to be observed rather sporadically within a much less intense continuous background (with $\sqrt{\langle B_w^2\rangle_t} \sim 20$ pT) [*Meredith et al.*, 2008, 2009; *Shprits et al.*, 2013]. Thus, lifetimes can be expected to be strongly reduced only during disturbed periods.

4.2. Effect on Electron Energization

[31] As concerns electron momentum diffusion, it is easy to compare the rates derived from equations (17)–(18) for fast magnetosonic waves, with the rates obtained previously for whistler-mode hiss or chorus waves [*Mourenas et al.*, 2012a]. Let us focus on large pitch angles $\alpha_0 > 45°$, which correspond to the majority of trapped particles. Additionally, it is assumed that $\alpha_0 > \pi/2 - \Delta\theta_{\mathrm{H}(CH)}$ and

$$\cos\alpha_0 > \frac{|1 - \gamma\omega_{m,\mathrm{H}(CH)}/\Omega_{ce0}|\sqrt{1 - \omega_{m,\mathrm{H}(CH)}/\Omega_{ce0}}}{p\varepsilon_{\mathrm{H}(CH)}} \quad (27)$$

When oblique chorus waves are present (as observed during relatively quiet periods such that $K_p < 3$) at $L = 4$ to 5.5 on the dayside, the ratio of fast magnetosonic to chorus momentum diffusion rates is

$$\frac{\langle D^{pp}\rangle_B}{\langle D_{CH}^{pp}\rangle_B} \approx \frac{4\Delta\lambda B_w^2 \tan^2\alpha_0 \Phi_0^2\, g(\theta_r)\, \Omega_{ci0}^{3/2} \tan^2\theta_m}{B_{w,CH}^2 \omega_m \Omega_{ce0}^{1/2} \tan\Delta\theta}, \quad (28)$$

while when comparing with moderately oblique hiss waves inside the plasmasphere, the ratio of momentum diffusion rates is

$$\frac{\langle D^{pp}\rangle_B}{\langle D_{\mathrm{H}}^{pp}\rangle_B} \approx \frac{1.5\Delta\lambda B_w^2 \tan^2\alpha_0 \Phi_0^2\, g(\theta_r)\, \Omega_{ci0}^{3/2} \tan^2\theta_m}{B_{w,\mathrm{H}}^2 \sin\alpha_0 \omega_m \omega_{m,\mathrm{H}}^{1/2} (\tan\Delta\theta/\tan\Delta\theta_{\mathrm{H}})}. \quad (29)$$

Taking $\alpha_0 = \alpha_{0M}$ to consider the (nearly) peak value of the momentum diffusion rate for magnetosonic waves, it is easy to show that both ratios increase with energy, reaching a maximum for energies such that Φ_0^2 is close to its peak, for $\sin\alpha_{0M}\gamma v/c \approx 1.8\Omega_{ce0}^{3/2}\Omega_{ci0}^{1/2}/(\Omega_{pe}\omega_m)$. At lower energy, they vary like $(\Omega_{pe}/\Omega_{ce0})^4$. While these wave power ratios are always inversely proportional to $\tan\Delta\theta$, the pitch angle width of the peak of magnetosonic wave momentum diffusion is itself proportional to $\Delta\theta$.

5. Comparisons With Full Numerical Simulations and Discussion

[32] We use the numerical scheme of calculation of diffusion rates described by [*Glauert and Horne*, 2005] to obtain $D_0^{\alpha\alpha}$ and D_0^{EE} for various values of system parameters (see details in section A). Numerical results serve as a validation of our analytical estimates.

[33] In Figure 3, the bounce-averaged pitch angle diffusion rate of electrons by fast magnetosonic waves given by equation (17) is compared with the full numerical solution for different energies, demonstrating the good precision of the analytical estimates. Here, an amplitude of 100 pT is considered at $L = 4.5$ (other parameters are as indicated in section 2). One can see that there is a good correspondence between numerical and analytical results even for large plasma density $\Omega_{pe}/\Omega_{ce0} = 10$. Expression (17) provides the maximum value of $D_0^{\alpha\alpha}$ and the position of this maximum α_{0M} with a good accuracy for energies from 100 keV up to 2 MeV.

[34] Next, the bounce-averaged pitch angle diffusion rate for various ion compositions of the plasma are shown in Figure 4 for two energies ($E = 300$ keV and 2 MeV). We consider four variants of plasma mixture: a purely proton-electron plasma, a small fraction of helium $\left(n_{\mathrm{H}_e^+}/n_e = 0.1\right)$,

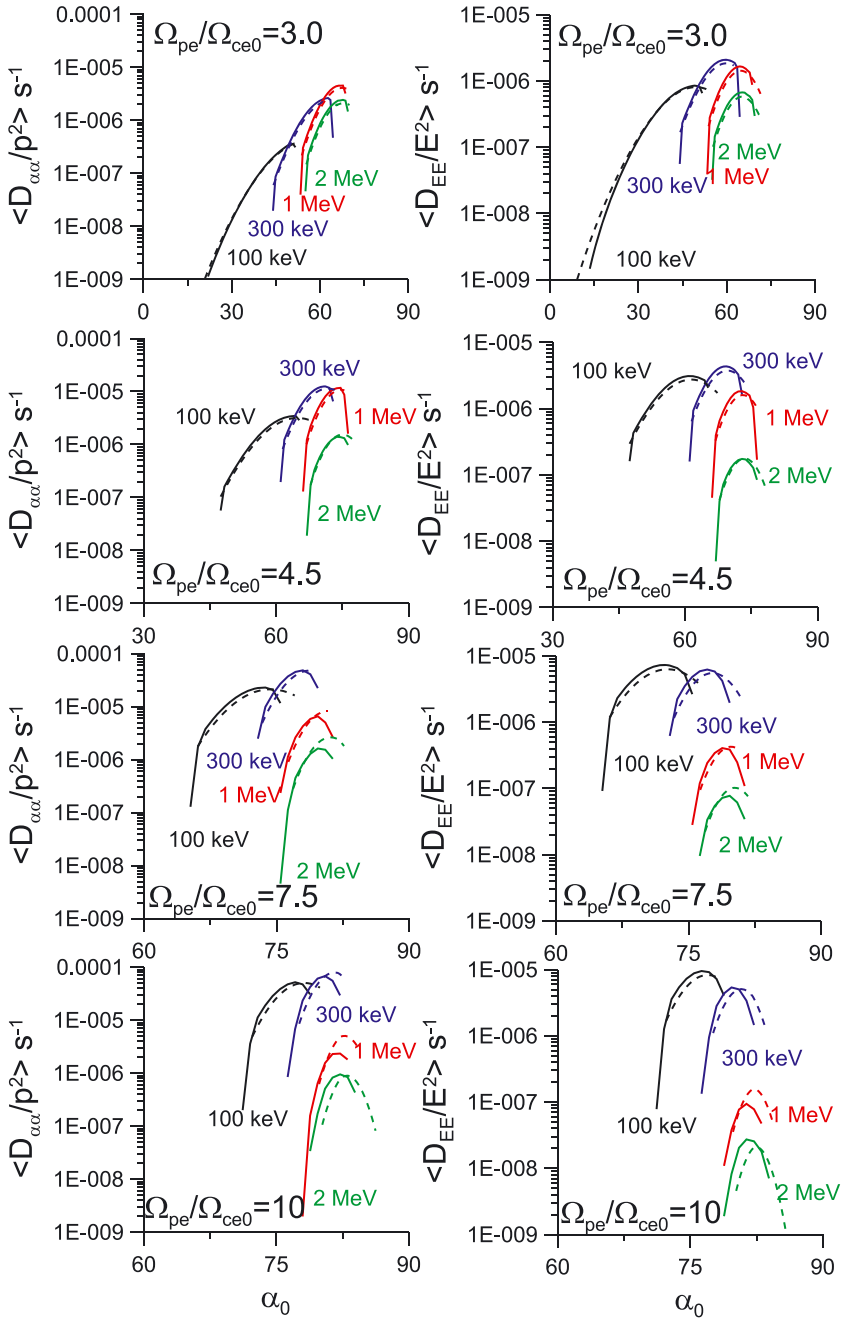

Figure 3. Pitch angle and energy diffusion coefficients for various values of Ω_{pe}/Ω_{ce0} and electron energy. Solid curves show full numerical solution, while dotted curves show analytical estimates (17).

helium-oxygen fractions with small (n_{O^+}/n_e = 0.1), and large (n_{O^+}/n_e = 0.2) oxygen populations. For small plasma density $\Omega_{pe}/\Omega_{ce0} \leq 5$, the numerical solution is again well reproduced by the analytical formula. There is a certain discrepancy between numerical results and analytical estimates for large plasma density $\Omega_{pe}/\Omega_{ce0} > 5$. Nevertheless, the discrepancy concerning the position of the maximum diffusion rate remains less than 2°. Maximum analytical diffusion rates are always in very good agreement with full numerical values at low energies $E < 1$ MeV, and they still remain within a factor of 2 of actual values at higher energies.

[35] The peak values (for $\alpha_0 = \alpha_{0M}$) of the analytical pitch angle and energy diffusion rates by fast magnetosonic waves are displayed in Figures 5 and 6 as a function of the main wave parameters, i.e., the normalized mean frequency ω_m/Ω_{ci0}, the mean wave-normal angle θ_m, and the corresponding width $\Delta\theta$, which are determining the magnitude of diffusion rates in equation (17). The other (plasma) parameters have been selected to correspond to typical conditions at $L = 4.5$ and $L = 2$. A maximum of diffusion at relatively small ω_m/Ω_{ci0} (i.e., the lower band of fast magnetosonic waves) is observed in Figure 5. As explained above, it corresponds to the parameter range where $\Phi_0^2 \sim J_1^2$ is near its peak value, i.e., for $\omega_m/\Omega_{ci0} \sim \sqrt{\Omega_{ce0}/\Omega_{ci0}}(\Omega_{ce0}/\Omega_{pe})c/(\gamma v)$. Stronger diffusion obtains also for mean wave-normal angle $\theta_m < 89.2°$ for energies

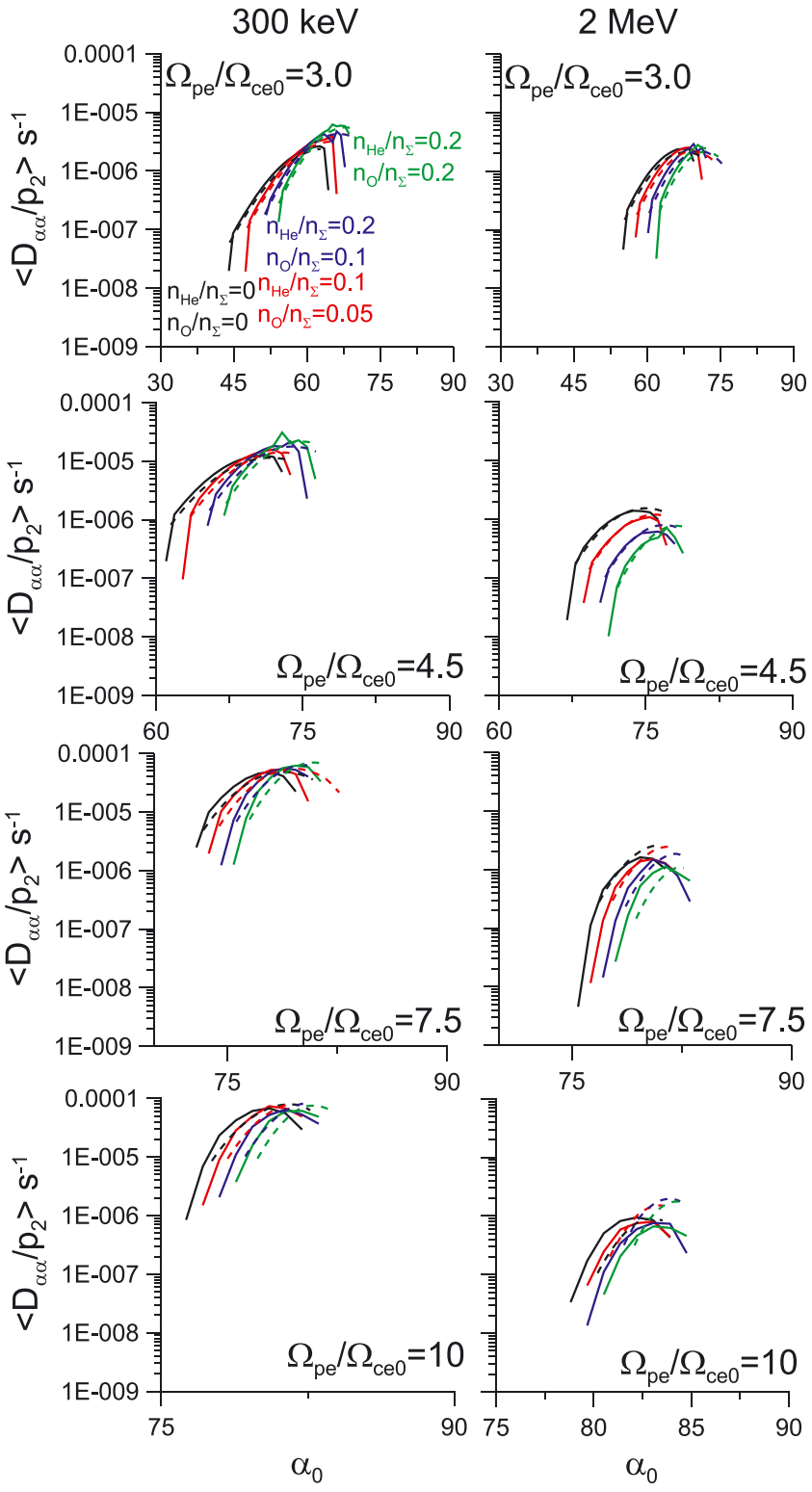

Figure 4. Pitch angle diffusion coefficients for various values of Ω_{pe}/Ω_{ce0}, ion composition, and electron energy. Solid curves show full numerical solution, while dotted curves show analytical estimates (17).

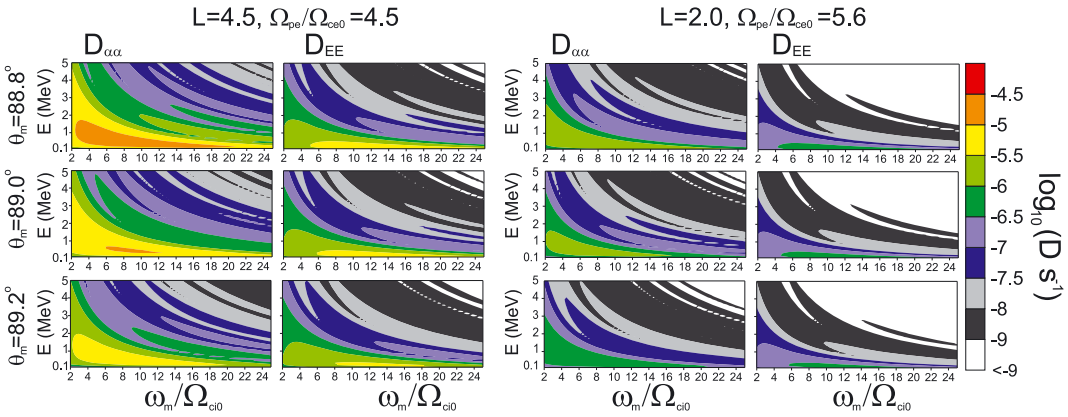

Figure 5. Maximum analytical bounce-averaged pitch angle and energy diffusion rates of electrons by fast magnetosonic waves, as a function of normalized mean frequency ω_m/Ω_{ci0} and electron energy, for different values of the mean wave-normal angle θ_m and Ω_{pe}/Ω_{ce0}. Here $\Delta\theta = 86°$ and $B_w = 100$ pT.

$E > 0.3$ MeV. As shown in Figure 6, the diffusion rates decrease with increasing $\Delta\theta$ like $1/\tan\Delta\theta$. On the other hand, the width of the pitch angle range of significant diffusion increases with $\Delta\theta$ (see equation (19) and Figure 6), with a very slight influence of the frequency width $\Delta\omega$ as long as $\omega_m\Delta\omega \ll \Omega_{ce0}\Omega_{ci0}$. Likewise, the magnitude of the analytical diffusion rate is independent of $\Delta\omega$. But we must recall here that the analytical expression (17) has been derived for not-too-narrow frequency distributions such that $\Delta\omega/\omega_m > 0.15$.

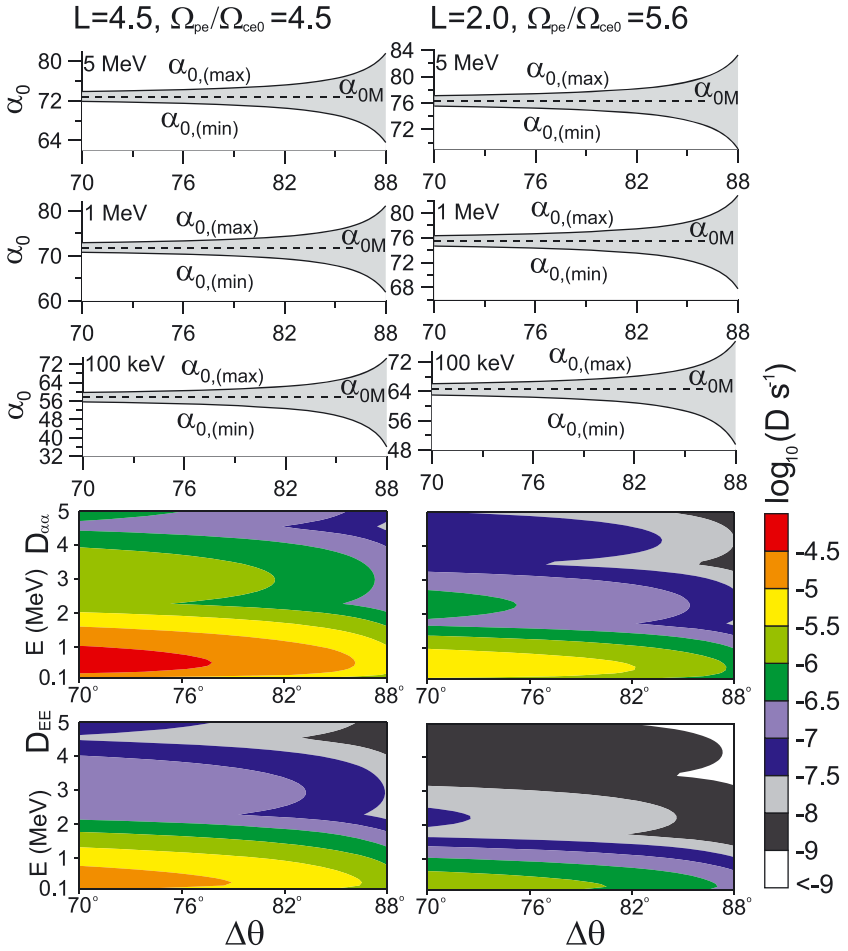

Figure 6. Top panels show α_0 ranges of significant diffusion from equation (19), while bottom panels show maximum analytical bounce-averaged pitch angle and energy diffusion rates of electrons by fast magnetosonic waves, as a function of wave-normal angle width $\Delta\theta$ of the distribution, for different energies and Ω_{pe}/Ω_{ce0} ratios. Here $\omega_m/\Omega_{ci0} = 7$, $\theta_m = 89°$, and $B_w = 100$ pT.

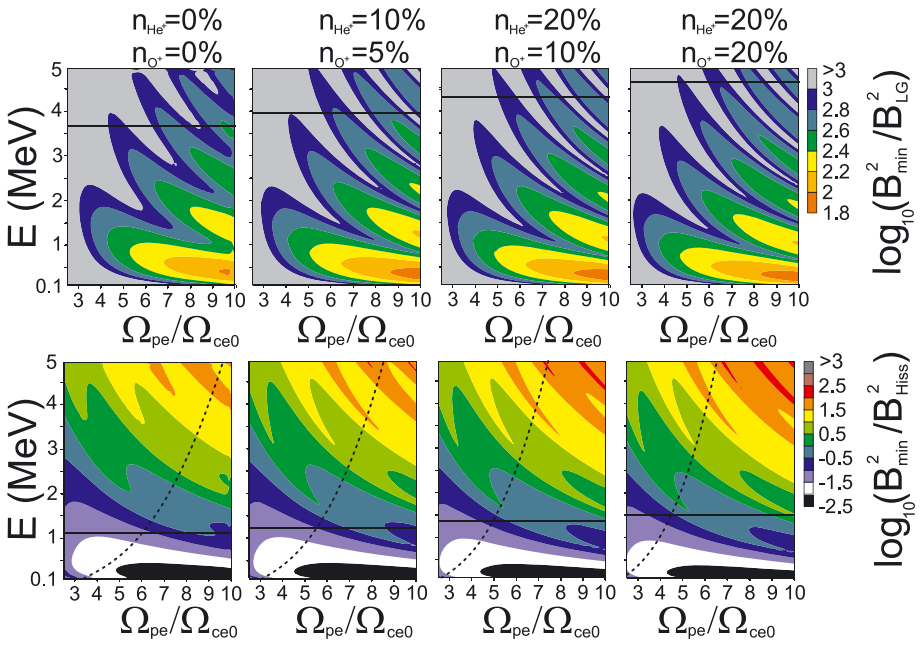

Figure 7. Minimum fast magnetosonic to lightning-generated wave intensity ratio (21) needed for pitch angle diffusion by magnetosonic waves to be comparable to, or larger than, diffusion by lightning-generated waves, as a function of electron energy and Ω_{pe}/Ω_{ce0} (top panels). Minimum fast magnetosonic to hiss wave intensity ratio (22) required for magnetosonic waves to yield larger pitch angle diffusion rates than hiss waves, as a function of electron energy and Ω_{pe}/Ω_{ce0} (bottom panels). Various ion compositions of the plasma are considered. Parameter domains of strong potential effect of magnetosonic waves on lifetimes are delimited by solid and dashed lines (see text for details).

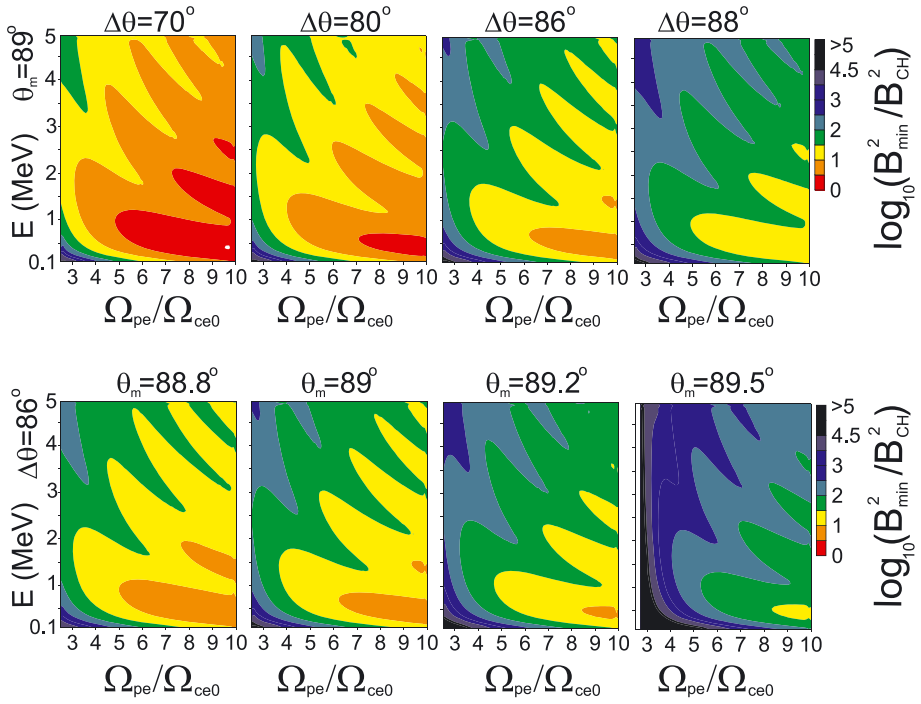

Figure 8. Minimum fast magnetosonic to chorus wave intensity ratio (20) needed for pitch angle diffusion by magnetosonic waves to be comparable to, or larger than, diffusion by chorus waves, as a function of electron energy and Ω_{pe}/Ω_{ce0}. Different magnetosonic wave-normal angle distributions are considered by varying the mean value θ_m and the width $\Delta\theta$.

[36] Next, we plot in Figure 7 the ranges of potentially strong impact of fast magnetosonic waves on lifetimes, inside the plasmasphere (for $L = 2$) in the presence of hiss and lightning-generated waves. The magnitude of the minimum wave power ratios (21) and (22) is shown in color scale, while the parameter range of strong effect is delimited by dotted and solid black lines, for a typical hiss to lightning-generated waves power ratio of 60 and upper cutoffs of Hiss and lightning-generated waves at 900 Hz and 5 kHz [*Meredith et al.*, 2009; *Artemyev et al.*, 2013]. Conditions (24) and (25) are satisfied below the solid black lines and above the dotted lines. In the upper panels, note that the dotted lines are at $E = 0$. A lower hiss to lightning-generated wave power ratio (smaller than 10) would be needed to obtain lower bounds at $E > 0$ for strong effects of magnetosonic waves. It appears that magnetosonic waves may reduce lifetimes by filling the vicinity of the hiss Landau peak mainly for small density and energy. The density range of strong potential effect is also reduced for large percentages of heavy ions. Conversely, magnetosonic waves may have a strong influence at smaller pitch angles (where lightning-generated wave diffusion dominates) over a much broader parameter range, especially at high density and for $E = 0.2$ to 2 MeV in a pure proton-electron plasma, and at slightly lower energies when heavy ions are included. In general, the additional presence of heavy ions expected during the different phases of large geomagnetic storms [*Shprits et al.*, 2013] can be seen to mitigate the impact of magnetosonic waves if their intensities do not increase more than the other types of waves, except for some cases at low energy $E < 300$ keV.

[37] Figure 8 shows the minimum wave power ratio (20) in the presence of relatively oblique chorus waves outside of the plasmasphere as a function of $\Delta\theta$, θ_m and density, for $L = 4.5$. Although the magnitude of pitch angle diffusion increases strongly as $1/\tan\Delta\theta$ for smaller $\Delta\theta$, the overall effect on lifetimes should be small due to the simultaneous narrowing of the pitch angle range of significant diffusion. However, one can see that for small enough values of the mean wave-normal angle of fast magnetosonic waves, such that $\theta_m < 89°$, $B_w \sim B_{w,CH}$ is already enough to produce a sensible effect on particle scattering. This effect is especially strong for large plasma density $\Omega_{pe}/\Omega_{ce0} > 5$ and intermediate energies $0.25 < E(\mathrm{MeV}) < 2$.

[38] Next, Figure 9 shows two examples of small and strong effects of fast magnetosonic waves on lifetimes, as calculated from the full numerical solutions as well as by using the approximate formula (26). Realistic average wave intensities observed by CRRES at $L = 2$ during quiet periods are used: 22.5 pT hiss and 3 pT lightning-induced waves, for $\Omega_{pe}/\Omega_{ce0} = 5.6$ [*Meredith et al.*, 2009; *Artemyev et al.*, 2013]. Only small decreases of lifetimes are obtained for magnetosonic wave intensity equal to that of lightning-generated waves, which roughly corresponds in this case to average intensities of magnetosonic waves obtained from equation (1) on the basis of Cluster statistics. Moreover, lifetimes are slightly reduced only for $E \approx 1$ MeV, which compares well with the narrow domain of potential impact of magnetosonic waves predicted in the lower panel of Figure 7 for $\Omega_{pe}/\Omega_{ce0} \sim 5$–6. It corresponds to a very moderate filling of the minimum in diffusion rate between the cyclotron peak from lightning-generated waves and the Landau peak from

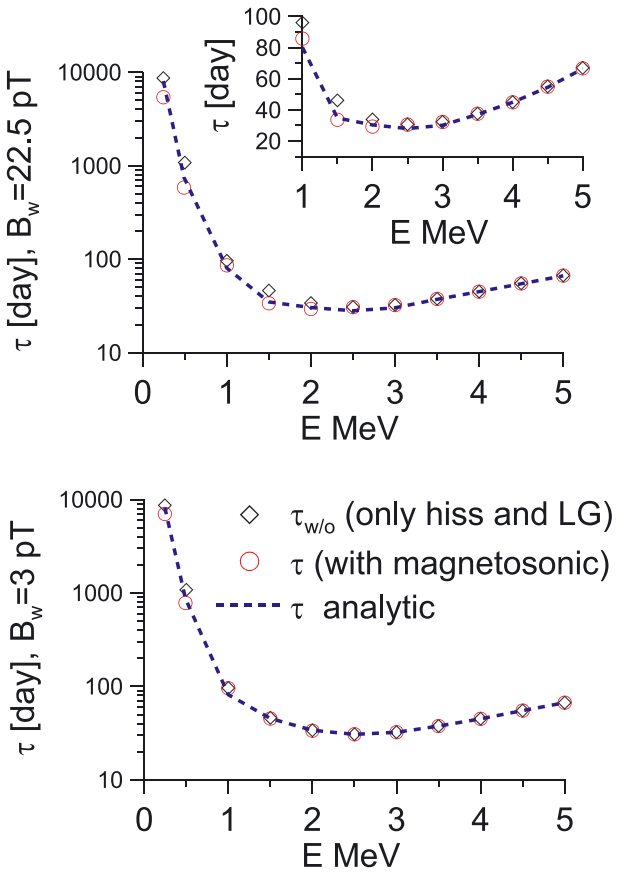

Figure 9. Lifetimes for $L = 2$. Two cases are considered: with magnetosonic wave amplitudes equal to hiss amplitudes (top panel) and with small amplitudes of magnetosonic waves (bottom panel). Insert figure in top panel shows same data but for a smaller energy range.

hiss waves. When fast magnetosonic waves reach higher intensities similar to hiss, a much more important reduction of lifetimes is observed (see upper panel of Figure 9), as expected from Figure 7 (upper panel) since the ratio of magnetosonic to lightning-generated waves intensities has been increased from 1 to ~ 60. In further agreement with Figure 7 (see also *Meredith et al.* [2009]), the main impact is obtained at small energies (for $E \sim 0.25$ to 2 MeV). In this case, the level of magnetosonic waves becomes high enough to sensibly increase pitch angle diffusion even in the domain $\alpha_0 < \alpha_{UC,\mathrm{LG}}$ corresponding to lightning-generated whistler-mode waves, as demonstrated in the lower panel of Figure 10 for the same parameters.

[39] The analytical expression (26) can be seen in Figure 9 to provide a good quantitative estimate of the reduction of lifetimes. Thus, we can conclude that for the final calculation of the effect of fast magnetosonic waves, one can simply use the numerical results for hiss and lightning-generated waves together with equation (26). It is especially important for the calculation of trapped electron lifetimes in the plasmasphere, where statistical information about magnetosonic waves is still relatively poor and the corresponding calculations should be performed over a wide range of system parameters. Our analytical estimates can also be used

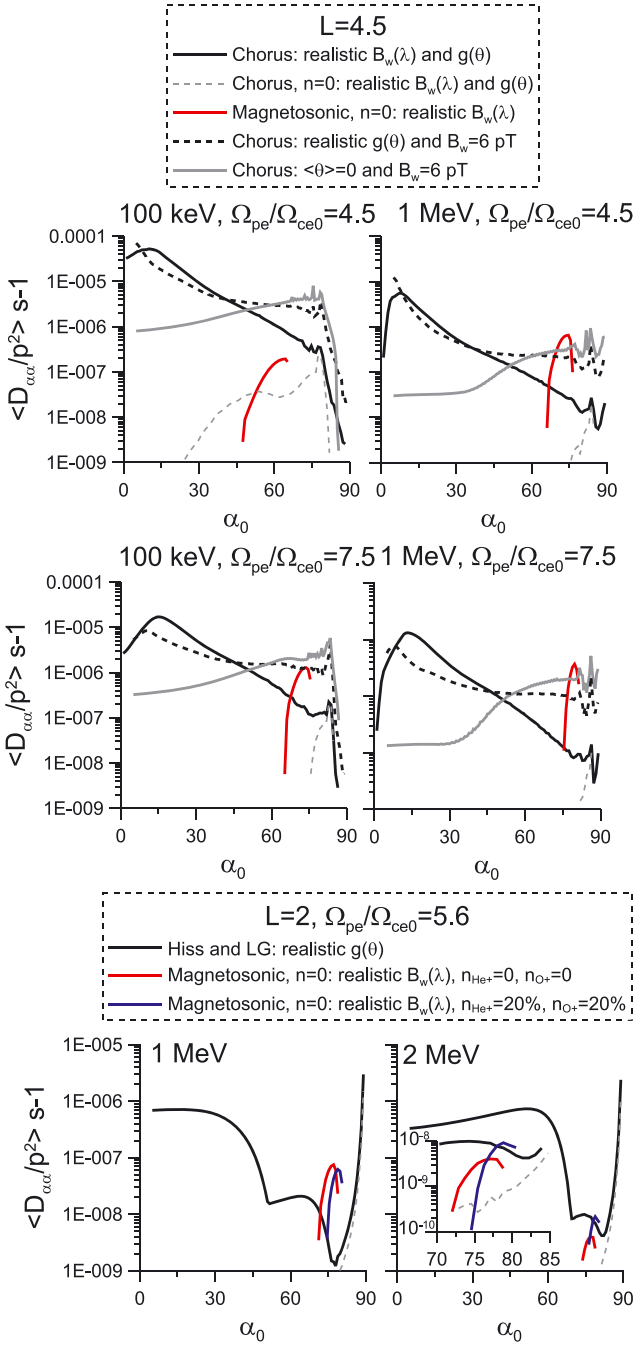

Figure 10. Diffusion coefficients for L = 4.5 and L = 2.0. For L = 4.5, quiet-time chorus wave amplitudes are taken according to Cluster statistics [see *Artemyev et al.*, 2013], while magnetosonic wave amplitudes are taken from equation (1). For L = 2.0, quiet-time hiss and lightning wave amplitudes from CRRES data are used [see *Artemyev et al.*, 2013; *Meredith et al.*, 2009], while magnetosonic wave amplitudes are assumed to be equal to hiss amplitudes [see *Meredith et al.*, 2009].

simply to evaluate the sensitivity of the results of radiation belt simulations to the potential perturbation induced by fast magnetosonic waves of a given level in the period of interest.

[40] Figure 10 shows in detail the full numerical diffusion coefficients for magnetosonic waves, chorus and hiss, outside and inside the plasmasphere, respectively. Here, the average magnetosonic wave intensity measured by Cluster is used for L = 4.5 (corresponding to much less intense events than the one treated by *Horne et al.* [2007]), while for L = 2.0 we assume that magnetosonic wave amplitude is equal to the amplitude of hiss [see *Meredith et al.*, 2009], corresponding to the case of Figure 9. Typical dayside quiet-time chorus and hiss intensities are used [see *Artemyev et al.*, 2013]. The potential impact of magnetosonic waves on lifetimes in the outer belt (the case at L = 4.5) appears more important for electron energies around 1 MeV than at low energy (< 250 keV) and also more significant at higher density Ω_{pe}/Ω_{ce0} > 5, in agreement with Figure 8. Note, however, that we use in our analytical estimates of chorus diffusion rates a constant (average) intensity of chorus waves as a function of latitude. As shown in Figure 10 (compare heavy solid and dashed black lines in upper panels), using a realistic latitudinal variation of chorus intensity from Cluster measurements on the dayside would actually increase the effect of magnetosonic waves. This stems from a minimum in measured amplitudes of chorus in Cluster statistics near the equator, especially on the dayside [*Artemyev et al.*, 2013]. Real, MLT-averaged chorus diffusion rates are expected to lie between the constant intensity rates and the latitude-varying intensity rates, because of higher amplitudes near the equator as well as lower obliquity of chorus waves on the nightside [*Agapitov et al.*, 2011, 2012; *Artemyev et al.*, 2013]. Anyway, including magnetosonic waves with their average intensities is seen to increase diffusion at large pitch angles, reducing lifetimes (by factors ~2) and making the actual, total diffusion rates much closer to the dayside chorus diffusion rates calculated for constant (average) chorus intensities as a function of latitude (which actually correspond to our analytical estimates for chorus; see *Mourenas et al.* [2012b] and *Artemyev et al.* [2013]).

[41] At L = 2, conversely, average magnetosonic wave intensities from Cluster lead to a 30% reduction of lifetimes at most in the presence of average hiss and lightning-generated waves. Only for lower-than-average plasma density or for higher amplitudes of magnetosonic waves closer to hiss amplitudes can a more sensible decrease of lifetimes eventually occur. Since equation (1) shows that measured magnetosonic wave average intensities increase exponentially toward L = 4.5, one expects magnetosonic waves to reduce lifetimes much more sensibly at larger L shells in the plasmasphere, closer to the plasmapause. In the slot region, only very intense magnetosonic wave events, with intensities much higher than the values obtained after averaging over years of measurements, will significantly impact lifetimes. Nevertheless, magnetosonic wave levels similar to hiss are still realistic even at L = 2 [*Meredith et al.*, 2009]. Similar intensities have indeed been observed on Cluster at L ~ 2.5 at MLT 12–18 after averaging over years of measurements (see Figure 2a). Moreover, Cluster data at L < 2.5 are really scarce, which probably leads to an underestimation of magnetosonic wave amplitudes there. It means

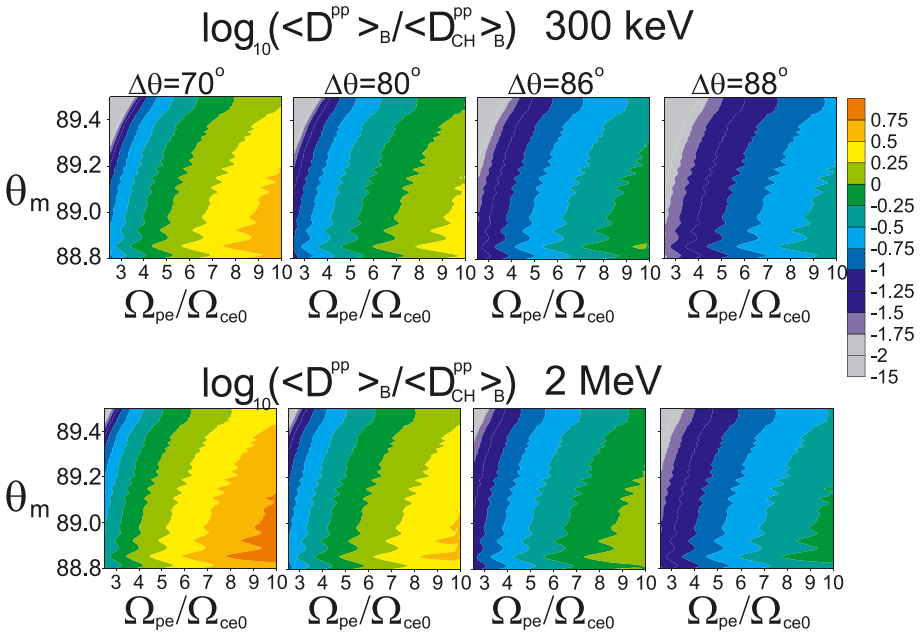

Figure 11. Ratio of fast magnetosonic to chorus momentum diffusion coefficients given by equation (28) for $L = 4.5$ ($B_w \approx 25$ pT, $B_{w,CH} \approx 6$ pT).

that intensity levels (averaged over MLT) similar to hiss will probably be observed during 1 or 2 days each month at $L = 2$, even during quiet periods. Thus, fast magnetosonic waves could play the same role as VLF waves from ground transmitters in reducing electron lifetimes in the range $L = 2$ to 4 inside the plasmasphere but only during short periods of time at $L < 3$. A more precise statistical survey of magnetosonic wave intensity variations at low L is needed to examine this point in a more comprehensive way.

[42] Last, Figure 11 shows the ratio of magnetosonic to chorus analytical momentum diffusion rates at $L = 4.5$ as a function of magnetosonic wave parameters $\Delta\theta$ and θ_m as well as density for $\alpha_0 = \alpha_{0M}$. Here, the quiet-time magnetosonic and chorus average intensities measured by Cluster are used. The effect on electron energization may be stronger for narrow wave-normal distributions of fast magnetosonic waves but only over a reduced pitch angle range (proportional to $\Delta\theta$). Electron energization is also slightly increased as the mean value θ_m decreases from 89.5°. Finally, the effects of average-intensity fast magnetosonic waves on momentum diffusion could become significant in regions of high Ω_{pe}/Ω_{ce0} ratio and for $E > 100$ keV during quiet periods. But their impact on electron acceleration should be especially important during very intense magnetosonic wave events, like the one treated by *Horne et al.* [2007].

6. Conclusions

[43] In this paper, new simplified analytical expressions of the pitch angle and momentum quasi-linear diffusion rates of magnetospheric electrons in the presence of fast magnetosonic waves have been presented. The accuracy of the simplified formulas has been checked by means of full numerical calculations, demonstrating their good precision over a wide parameter range between 100 keV and 2 MeV at least. Moreover, the analytical estimates have been used together with previous analytical estimates of diffusion coefficients corresponding to scattering by chorus, hiss, and lightning-generated whistler-mode waves in order to determine the wave and plasma parameter domains where the effects of fast magnetosonic waves on electron lifetime or energization should be most important. An analytical estimate of the modified lifetime has also been provided, which compares well with full numerical results.

[44] When fast magnetosonic waves are competing with oblique chorus or with lightning-generated waves, a relatively smaller ($\leq 89°$) mean wave-normal angle of magnetosonic waves is more favorable, as well as higher plasma densities (or more precisely, a higher ratio $\Omega_{pe}/\Omega_{ce0} > 5$). Conversely, a relatively higher ($> 89°$) mean wave-normal angle and smaller densities are more propitious when fast magnetosonic waves are vying with plasmaspheric hiss. In all cases, an optimum value of the mean frequency of magnetosonic waves has been found, which mainly depends on plasma and energy parameters. It can be rewritten under the form $\omega_m/\Omega_{ci0} \sim \sqrt{\Omega_{ce0}/\Omega_{ci0}}(\Omega_{ce0}/\Omega_{pe})c/(\gamma v)$, leading to $\omega_m/\Omega_{ci0} \sim 25\Omega_{ce0}/\Omega_{pe} \leq 10$ for $E > 0.5$ MeV. It corresponds to the lower band of observed fast magnetosonic waves. A significant reduction of lifetimes has been obtained for realistic intensities of the different kinds of waves, pointing to the need of further experimental and numerical studies of fast magnetosonic waves to better ascertain their wave-normal and frequency distributions as well as to obtain a more precise statistics of their intensities as a function of geomagnetic activity.

Appendix A: Numerical Scheme

[45] For numerical calculation of diffusion coefficients, we use a more precise dispersion relation including ion terms [e.g., *Shklyar et al.*, 2004]:

$$\omega^2 = \Omega_{ce}^2 \Xi^2 \cos^2\theta + \Omega_{ce}\Omega_{ci}\Xi,$$

where $\Xi = (1 + (\Omega_{pe}/kc)^2)^{-1}$. For $\theta \sim 90°$, this relation transforms to equation (7). The corresponding derivatives are

$$\left.\frac{\partial\omega}{\partial k_\parallel}\right|_\theta = \frac{1}{2\omega}\frac{\partial\omega^2}{\partial k} = \frac{\Omega_{pe}^2\Omega_{ce}^2}{\omega k^3 c^2}\left(2\Xi^3\cos^2\theta + \frac{\Omega_{ci}}{\Omega_{ce}}\Xi^2\right). \quad \text{(A1)}$$

The simplified form of $\partial\omega/\partial k_\parallel|_\theta$ is

$$\left.\frac{\partial\omega}{\partial k_\parallel}\right|_\theta \approx \frac{c^2 k\Omega_{ce}\Omega_{ci}\Xi^2}{\omega\Omega_{pe}^2\cos\theta} = \frac{v_A\Xi^{3/2}}{\cos\theta} = \frac{v_A\Xi^{3/2}}{\cos\theta},$$

and corresponding ratio $(\partial\omega/\partial k_\parallel)/v_\parallel$ coincides with equation (12) for $v_\parallel = \omega/k\cos\theta$.

[46] The equation for resonant roots for $n = 0$ has the form

$$(kc)^2u^2 = \Omega_{ce}^2\Xi^2\cos^2\theta + \Omega_{ce}\Omega_{ci}\Xi, \quad \text{(A2)}$$

where $u = v_\parallel\cos\theta/c$. Here we use equation (A2) with constant plasma frequency $\Omega_{pe} = const$.

[47] We substitute expression (A1) and solutions of equation (A2) into equation (2) to calculate numerical diffusion coefficient for $n = 0$, $D_0^{\alpha\alpha}$. Averaging over latitude is performed according to *Lyons et al.* [1972]:

$$\langle D^{\alpha\alpha}\rangle_B = \frac{1}{T}\int_0^{\lambda_m}\frac{D^{\alpha\alpha}\cos\alpha\cos^7\lambda\,\mathrm{d}\lambda}{\cos^2\alpha_0}$$

$$\langle D^{pp}\rangle_B = \frac{1}{T}\int_0^{\lambda_m}\frac{D^{pp}\sqrt{1+3\sin^2\lambda}\cos\lambda\,\mathrm{d}\lambda}{\cos\alpha},$$

where $\lambda_m = \min(\lambda_{\mathrm{mir}}, \lambda_{\max})$ and λ_{mir} is the latitude of mirror points. To calculate D^{pp}, one should change expression (3) to

$$\Delta_n = \frac{\pi\Phi_n^2}{2\cos\theta|v_\parallel/c|^3}\frac{(\sin\alpha\cos\alpha)^2}{|1-(\partial\omega/\partial k_\parallel)_\theta/v_\parallel|}.$$

[48] **Acknowledgments.** The work of A.A.V. was partially supported by The Ministry of education and science of Russian Federation, project 8527.

[49] Robert Lysak thanks the reviewers for their assistance in evaluating this paper.

References

Agapitov, O., V. Krasnoselskikh, Y. V. Khotyaintsev, and G. Rolland (2011), A statistical study of the propagation characteristics of whistler waves observed by Cluster, *Geophys. Res. Lett.*, *382*, L20103, doi:10.1029/2011GL049597.

Agapitov, O., V. Krasnoselskikh, Y. V. Khotyaintsev, and G. Rolland (2012), Correction to "A statistical study of the propagation characteristics of whistler waves observed by Cluster", *Geophys. Res. Lett.*, *39*, L24102, doi:10.1029/2012GL054320.

Albert, J. M. (2005), Evaluation of quasi-linear diffusion coefficients for whistler mode waves in a plasma with arbitrary density ratio, *J. Geophys. Res.*, *110*, A03218, doi:10.1029/2004JA010844.

Albert, J. M. (2007), Simple approximations of quasi-linear diffusion coefficients, *J. Geophys. Res.*, *112*, A12202, doi:10.1029/2007JA012551.

Albert, J. M. (2008), Efficient approximations of quasi-linear diffusion coefficients in the radiation belts, *J. Geophys. Res.*, *113*, A06208, doi:10.1029/2007JA012936.

Albert, J. M., and Y. Y. Shprits (2009), Estimates of lifetimes against pitch angle diffusion, *J. Atmos. Sol. Terr. Phys.*, *71*, 1647–1652, doi:10.1016/j.jastp.2008.07.004.

Artemyev, A., O. Agapitov, H. Breuillard, V. Krasnoselskikh, and G. Rolland (2012), Electron pitch-angle diffusion in radiation belts: The effects of whistler wave oblique propagation, *Geophys. Res. Lett.*, *39*, L08105, doi:10.1029/2012GL051393.

Artemyev, A., D. Mourenas, O. Agapitov, and V. Krasnoselskikh (2013), Parametric validations of analytical lifetime estimates for radiation belt electron diffusion by whistler waves, *Ann. Geophys.*, *31*, 599–624, doi:10.5194/angeo-31-599-2013.

Balogh, A., et al. (2001), The Cluster Magnetic Field Investigation: Overview of in-flight performance and initial results, *Ann. Geophys.*, *19*, 1207–1217, doi:10.5194/angeo-19-1207-2001.

Barker, A. B., X. Li, and R. S. Selesnick (2005), Modeling the radiation belt electrons with radial diffusion driven by the solar wind, *Space Weather*, *3*, S10003, doi:10.1029/2004SW000118.

Boardsen, S. A., D. L. Gallagher, D. A. Gurnett, W. K. Peterson, and J. L. Green (1992), Funnel-shaped, low-frequency equatorial waves, *J. Geophys. Res.*, *97*, 14,967, doi:10.1029/92JA00827.

Bortnik, J., and R. M. Thorne (2010), Transit time scattering of energetic electrons due to equatorially confined magnetosonic waves, *J. Geophys. Res.*, *115*, A07213, doi:10.1029/2010JA015283.

Chen, L., R. M. Thorne, V. K. Jordanova, M. F. Thomsen, and R. B. Horne (2011), Magnetosonic wave instability analysis for proton ring distributions observed by the LANL magnetospheric plasma analyzer, *J. Geophys. Res.*, *116*, A03223, doi:10.1029/2010JA016068.

Chen, L., R. M. Thorne, W. Li, and J. Bortnik (2013), Modeling the wave normal distribution of chorus waves, *J. Geophys. Res. Space Physics*, *118*, 1074–1088, doi:10.1029/2012JA018343.

Choi, H.-S., et al. (2011), Analysis of GEO spacecraft anomalies: Space weather relationships, *Space Weather*, *9*, S06001, doi:10.1029/2010SW000597.

Cornilleau-Wehrlin, N., et al. (2003), First results obtained by the Cluster STAFF experiment, *Ann. Geophys.*, *21*, 437–456, doi:10.5194/angeo-21-437-2003.

Davidson, G. T. (1976), An improved empirical description of the bounce motion of trapped particles, *J. Geophys. Res.*, *81*, 4029, doi:10.1029/JA081i022p04029.

Fok, M.-C., A. Glocer, Q. Zheng, R. B. Horne, N. P. Meredith, J. M. Albert, and T. Nagai (2011), Recent developments in the radiation belt environment model, *J. Atmos. Sol. Terr. Phys.*, *73*, 1435–1443, doi:10.1016/j.jastp.2010.09.033.

Glauert, S. A., and R. B. Horne (2005), Calculation of pitch angle and energy diffusion coefficients with the PADIE code, *J. Geophys. Res.*, *110*, A04206, doi:10.1029/2004JA010851.

Gurnett, D. A. (1976), Plasma wave interactions with energetic ions near the magnetic equator, *J. Geophys. Res.*, *81*, 2765–2770, doi:10.1029/JA081i016p02765.

Horne, R. B., G. V. Wheeler, and H. S. C. K. Alleyne (2000), Proton and electron heating by radially propagating fast magnetosonic waves, *J. Geophys. Res.*, *105*, 27,597–27,610, doi:10.1029/2000JA000018.

Horne, R. B., R. M. Thorne, S. A. Glauert, N. P. Meredith, D. Pokhotelov, and O. Santolík (2007), Electron acceleration in the Van Allen radiation belts by fast magnetosonic waves, *Geophys. Res. Lett.*, *34*, 17,107, doi:10.1029/2007GL030267.

Iucci, N., et al. (2005), Space weather conditions and spacecraft anomalies in different orbits, *Space Weather*, *3*, S01001, doi:10.1029/2003SW000056.

Kasahara, Y., H. Kenmochi, and I. Kimura (1994), Propagation characteristics of the ELF emissions observed by the satellite Akebono in the magnetic equatorial region, *Radio Sci.*, *29*, 751–767, doi:10.1029/94RS00445.

Kim, K.-C., Y. Shprits, D. Subbotin, and B. Ni (2011), Understanding the dynamic evolution of the relativistic electron slot region including radial and pitch angle diffusion, *J. Geophys. Res.*, *116*, A10214, doi:10.1029/2011JA016684.

Laakso, H., H. Junginger, R. Schmidt, A. Roux, and C. de Villedary (1990), Magnetosonic waves above fc(H+) at geostationary orbit—GEOS 2 results, *J. Geophys. Res.*, *95*, 10,609–10,621, doi:10.1029/JA095iA07p10609.

Li, W., Y. Y. Shprits, and R. M. Thorne (2007), Dynamic evolution of energetic outer zone electrons due to wave-particle interactions during storms, *J. Geophys. Res.*, *112*, A10220, doi:10.1029/2007JA012368.

Liu, K., S. P. Gary, and D. Winske (2011), Excitation of magnetosonic waves in the terrestrial magnetosphere: Particle-in-cell simulations, *J. Geophys. Res.*, *116*, A07212, doi:10.1029/2010JA016372.

Lyons, L. R. (1974), Pitch angle and energy diffusion coefficients from resonant interactions with ion-cyclotron and whistler waves, *J. Plasma Phys.*, *12*, 417–432, doi:10.1017/S002237780002537X.

Lyons, L. R., R. M. Thorne, and C. F. Kennel (1971), Electron pitch-angle diffusion driven by oblique whistler-mode turbulence, *J. Plasma Phys.*, *6*, 589–606, doi:10.1017/S0022377800006310.

Lyons, L. R., R. M. Thorne, and C. F. Kennel (1972), Pitch-angle diffusion of radiation belt electrons within the plasmasphere, *J. Geophys. Res.*, *77*, 3455–3474, doi:10.1029/JA077i019p03455.

Meredith, N. P., R. B. Horne, and R. R. Anderson (2008), Survey of magnetosonic waves and proton ring distributions in the Earth's inner magnetosphere, *J. Geophys. Res.*, *113*, A06213, doi:10.1029/2007JA012975.

Meredith, N. P., R. B. Horne, S. A. Glauert, D. N. Baker, S. G. Kanekal, and J. M. Albert (2009), Relativistic electron loss timescales in the slot region, *J. Geophys. Res.*, *114*, A03222, doi:10.1029/2008JA013889.

Millan, R. M., and D. N. Baker (2012), Acceleration of particles to high energies in Earth's radiation belts, *Space Sci. Rev.*, *173*, 103–131, doi:10.1007/s11214-012-9941-x.

Mourenas, D., and J.-F. Ripoll (2012), Analytical estimates of quasi-linear diffusion coefficients and electron lifetimes in the inner radiation belt, *J. Geophys. Res.*, *117*, A01204, doi:10.1029/2011JA016985.

Mourenas, D., A. Artemyev, O. Agapitov, and V. Krasnoselskikh (2012a), Acceleration of radiation belts electrons by oblique chorus waves, *J. Geophys. Res.*, *117*, A10212, doi:10.1029/2012JA018041.

Mourenas, D., A. V. Artemyev, J.-F. Ripoll, O. V. Agapitov, and V. V. Krasnoselskikh (2012b), Timescales for electron quasi-linear diffusion by parallel and oblique lower-band Chorus waves, *J. Geophys. Res.*, *117*, A06234, doi:10.1029/2012JA017717.

Němec, F., O. Santolík, K. Gereová, E. Macúšová, Y. de Conchy, and N. Cornilleau-Wehrlin (2005), Initial results of a survey of equatorial noise emissions observed by the Cluster spacecraft, *Planet. Space Sci.*, *53*, 291–298, doi:10.1016/j.pss.2004.09.055.

Perraut, S., A. Roux, P. Robert, R. Gendrin, J.-A. Sauvaud, J.-M. Bosqued, G. Kremser, and A. Korth (1982), A systematic study of ULF waves above F_{H^+} from GEOS 1 and 2 measurements and their relationships with proton ring distributions, *J. Geophys. Res.*, *87*, 6219–6236, doi:10.1029/JA087iA08p06219.

Pokhotelov, D., F. Lefeuvre, R. B. Horne, and N. Cornilleau-Wehrlin (2008), Survey of ELF-VLF plasma waves in outer radiation belt observed by Cluster STAFF-SA experiment, *Ann. Geophys.*, *26*, 3269–3277, doi:10.5194/angeo-26-3269-2008.

Reeves, G. D., et al. (2012), Dynamic Radiation Environment Assimilation Model: DREAM, *Space Weather*, *10*, S03006, doi:10.1029/2011SW000729.

Russell, C. T., R. E. Holzer, and E. J. Smith (1970), OGO 3 observations of ELF noise in the magnetosphere: 2. The nature of the equatorial noise, *J. Geophys. Res.*, *75*, 755, doi:10.1029/JA075i004p00755.

Santolík, O., J. S. Pickett, D. A. Gurnett, M. Maksimovic, and N. Cornilleau-Wehrlin (2002), Spatiotemporal variability and propagation of equatorial noise observed by Cluster, *J. Geophys. Res.*, *107*, 1495, doi:10.1029/2001JA009159.

Santolík, O., M. Parrot, and F. Lefeuvre (2003), Singular value decomposition methods for wave propagation analysis, *Radio Sci.*, *38*, 1010, doi:10.1029/2000RS002523.

Shapiro, V. D., and R. Z. Sagdeev (1997), Nonlinear wave-particle interaction and conditions for the applicability of quasilinear theory, *Phys. Rep.*, *283*, 49–71.

Shklyar, D., J. Chum, and F. Jirícek (2004), Characteristic properties of Nu whistlers as inferred from observations and numerical modelling, *Ann. Geophys.*, *22*, 3589–3606, doi:10.5194/angeo-22-3589-2004.

Shprits, Y. Y., D. A. Subbotin, N. P. Meredith, and S. R. Elkington (2008), Review of modeling of losses and sources of relativistic electrons in the outer radiation belt II: Local acceleration and loss, *J. Atmos. Sol. Terr. Phys.*, *70*, 1694–1713, doi:10.1016/j.jastp.2008.06.014.

Shprits, Y. Y., A. Runov, and B. Ni (2013), Gyro-resonant scattering of radiation belt electrons during the solar minimum by fast magnetosonic waves, *J. Geophys. Res.*, *118*, 648–652, doi:10.1002/jgra.50108.

Stix, T. H. (1962), *The Theory of Plasma Waves*, McGraw-Hill, New York.

Summers, D. (2005), Quasi-linear diffusion coefficients for field-aligned electromagnetic waves with applications to the magnetosphere, *J. Geophys. Res.*, *110*, A08213, doi:10.1029/2005JA011159.

Summers, D., B. Ni, and N. P. Meredith (2007), Timescales for radiation belt electron acceleration and loss due to resonant wave-particle interactions: 1. Theory, *J. Geophys. Res.*, *112*, A04206, doi:10.1029/2006JA011801.

Thorne, R. M. (2010), Radiation belt dynamics: The importance of wave-particle interactions, *Geophys. Res. Lett.*, *372*, L22107, doi:10.1029/2010GL044990.

Ukhorskiy, A. Y., M. I. Sitnov, R. M. Millan, and B. T. Kress (2011), The role of drift orbit bifurcations in energization and loss of electrons in the outer radiation belt, *J. Geophys. Res.*, *116*, A09208, doi:10.1029/2011JA016623.

Varotsou, A., D. Boscher, S. Bourdarie, R. B. Horne, N. P. Meredith, S. A. Glauert, and R. H. Friedel (2008), Three-dimensional test simulations of the outer radiation belt electron dynamics including electron-chorus resonant interactions, *J. Geophys. Res.*, *113*, A12212, doi:10.1029/2007JA012862.

Xiao, F., Z. Su, H. Zheng, and S. Wang (2009), Modeling of outer radiation belt electrons by multidimensional diffusion process, *J. Geophys. Res.*, *114*, A03201, doi:10.1029/2008JA013580.